

AD-A038 540

HARRY DIAMOND LABS ADELPHI MD
A TENTATIVE MODEL OF THE SI-SIO₂ INTERFACE.(U)
FEB 77 M M SOKOLOSKI
HDL-TR-1787

F/G 9/1

UNCLASSIFIED

NL

1 OF 1
AD
A038 540



END
DATE
FILMED
10-77
DDC

HDL-TR-1787

A Tentative Model of the Si-SiO₂ Interface

February 1977

TR-1787—A Tentative Model of the Si-SiO₂ Interface, by Martin M. Solarski

AD-A038540

File Copy



U.S. Army Materiel Development
and Readiness Command
HARRY DIAMOND LABORATORIES
Adelphi, Maryland 20783

—
Replacement copy of HDL-TR-1787
Previous copy obsolete; please destroy.

The findings in this report are not to be construed as an official Department of the Army position unless so designated by other authorized documents.

Citation of manufacturers' or trade names does not constitute an official indorsement or approval of the use thereof.

Destroy this report when it is no longer needed. Do not return it to the originator.

UNCLASSIFIED

SECURITY CLASSIFICATION OF THIS PAGE (When Data Entered)

REPORT DOCUMENTATION PAGE		READ INSTRUCTIONS BEFORE COMPLETING FORM
1. REPORT NUMBER HDL-TR-1787	2. GOVT ACCESSION NO.	3. RECIPIENT'S CATALOG NUMBER
4. TITLE (and Subtitle) A Tentative Model of the Si-SiO ₂ Interface		5. TYPE OF REPORT & PERIOD COVERED Technical Report
7. AUTHOR(s) Martin M. Sokoloski		6. PERFORMING ORG. REPORT NUMBER
9. PERFORMING ORGANIZATION NAME AND ADDRESS Harry Diamond Laboratories 2800 Powder Mill Road Adelphi, MD 20783		8. CONTRACT OR GRANT NUMBER(s) DA: 1T161102AH44
11. CONTROLLING OFFICE NAME AND ADDRESS US Army Materiel Development & Readiness Command Alexandria, VA 22333		10. PROGRAM ELEMENT, PROJECT, TASK AREA & WORK UNIT NUMBERS Program Element: 6.11.02.A
14. MONITORING AGENCY NAME & ADDRESS (if different from Controlling Office)		12. REPORT DATE February 1977
		13. NUMBER OF PAGES 49
		15. SECURITY CLASS. (of this report) Unclassified
		15a. DECLASSIFICATION/DOWNGRADING SCHEDULE
16. DISTRIBUTION STATEMENT (of this Report) Approved for public release; distribution unlimited.		
17. DISTRIBUTION STATEMENT (of the abstract entered in Block 20, if different from Report)		
18. SUPPLEMENTARY NOTES HDL Project: A44628 DRCMS Code: 611102.11.H4400		
19. KEY WORDS (Continue on reverse side if necessary and identify by block number) Interface Band tails Heterojunction Capacitance-voltage measurement Disorder Fluctuating interface potential		
20. ABSTRACT (Continue on reverse side if necessary and identify by block number) A model of the electronic density of states in a metal-insulator-semiconductor structure is proposed. The model is based upon current theories of the electronic properties of amorphous materials and disordered alloys. The model accounts for the presence of "band-tail" states at the insulator-semiconductor interface and also speculates about the presence of states in the oxide as being due to persistent silicon conduction		

UNCLASSIFIED

SECURITY CLASSIFICATION OF THIS PAGE (When Data Entered)

and valence bands. The derivation of the admittance of a metal-oxide-semiconductor capacitor with a distribution of the interface states is reviewed, and an interpretation of these states employing the macroscopic theory of Brews is later derived. It is shown how these states can be measured by a quasi-static capacitance voltage measurement.

CONTENTS

	<u>Page</u>
1. INTRODUCTION	5
2. MICROSCOPIC THEORY	11
2.1 Intrinsic Interface States	11
2.2 Extrinsic Interface States	20
3. FORMULATION	21
3.1 Admittance for Distribution of Interface States	21
3.2 Fluctuations in Potential	29
3.3 Inclusion of Interface Potential Fluctuations on Admittance	33
4. QUASI-STATIC CAPACITANCE VOLTAGE METHOD FOR MEASUREMENT OF DENSITY OF INTERFACE STATES	38
4.1 Criteria for Reversibility	38
4.2 Determination of Various Parameters in Density of States Formulation	40
5. CONCLUSION	42
LITERATURE CITED	43
DISTRIBUTION	45

FIGURES

1 Metal-oxide-semiconductor capacitor	5
2 An n-channel metal-oxide-semiconductor field-effect transistor	6
3 One possible dependence of composition of graded A _x B _{1-x} heterojunction	13

FIGURES (Cont'd)

	<u>Page</u>
4 Possible dependence of density of states for alloy $A_x B_{1-x}$ heterojunction	14
5 Radial distribution curves for amorphous and crystalline Si as determined from analysis of electron diffraction data . . .	15
6 Metamorphosis of density of states from that in bulk SiO_2 to that in bulk Si	17
7 Heterogeneous model	18
8 Transition from glassy amorphous SiO_2 to crystalline Si state	19
9 Circuit for metal-oxide-semiconductor capacitor with discrete noninteracting bound states in insulator-semiconductor interface	27
10 Metal-oxide-semiconductor structure divided into two arbitrarily small areas of uniform charge density	30
11 Oxide-semiconductor interface	34

1. INTRODUCTION

Metal-insulator-semiconductor (MIS) structures and, in particular, those in which the insulator is an oxide of Si are being increasingly employed in both the civilian and military electronics markets. These structures are employed in a class of devices known as field effect transistors (FET's). When the FET consists of a metal-oxide-semiconductor (MOS) structure, it is then labeled MOSFET, or MOS device; insulated gate FET (IGFET) also occurs in the literature.

The MOS structure (fig. 1) is physically a semiconductor substrate (usually Si) on which is grown an oxide layer. Onto this is evaporated a thin metallic layer called the gate. The structure (sometimes called an MOS capacitor or diode) consists of a metal-insulator junction and an insulator-semiconductor junction. Since these junctions consist of two materials with a different band gap, they are called heterojunctions. In contrast, a p-n junction is a homojunction.

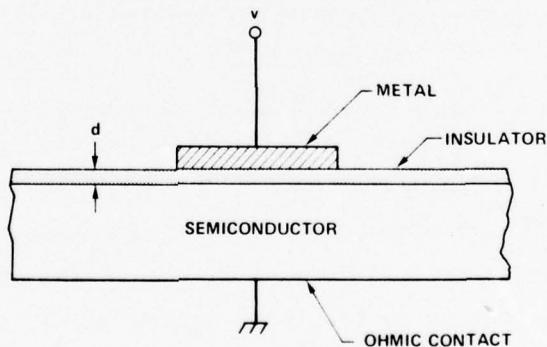


Figure 1. Metal-oxide-semiconductor capacitor.

The MOS structure is used mainly as a diagnostic tool to study phenomena associated with such heterojunctions. The actual useful device is the MOSFET (fig. 2). Before the oxide is grown on the

surface of the semiconductor substrate (p-type, fig. 2), two n+ regions called source and drain are diffused in the p-type bulk substrate (fig. 2). Ohmic contact is made to these, and a gate is then separated from the p-type bulk by an oxide layer. With no voltage on the gate, the current path from the source to the drain is effectively open. For the p-type bulk device, a positive voltage can be found whereby the electrons accumulate near the oxide-semiconductor interface and form a so-called inversion layer and short-circuit the source-drain electrodes. When a voltage difference is subsequently placed between the source and the drain, a current flows. The gate voltage at which this current flow begins is called the threshold voltage (V_T).

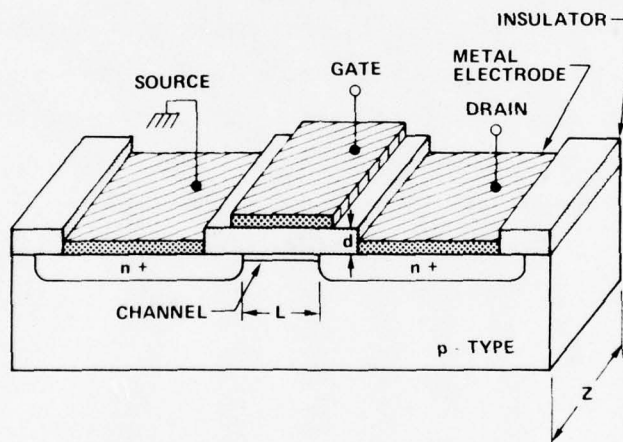


Figure 2. An n-channel metal-oxide-semiconductor field effect transistor.

There has been an extensive amount of experimental work on the nature of the oxide-semiconductor interface and, more specifically, the SiO_2 -Si interface. The interface is composed, on one hand, of an amorphous insulator with a forbidden energy gap of approximately 8 to 9 eV and, on the other hand, of a semiconductor with a gap of approximately 1.1 eV at 300 K. At the interface, there are two types of electronic states: (1) those that are in the oxide and do not communicate with either the metal or semiconductor electrode and (2) those that are in the Si forbidden gap and do communicate with the semiconductor electrode.

There are other complications with this MOS system. For instance, depending on the history of the device, mobile ions (in particular, Na^+) can exist in the oxide layer. With proper bias on the metal electrode and at elevated temperatures,* the ions can be asymmetrically distributed with the mean of the distribution being near the metal oxide or near the oxide semiconductor interface.¹ In each instance, the ions form a dipole layer near the interface and cause a lowering of the interface barrier. Also, segregation of the impurity dopant atoms that were formerly in the bulk Si can occur in the oxide near the oxide-semiconductor interface. This occurrence, in turn, can either enhance or decrease the polarization layer due to the former mobile ions such as Na^+ . In any case, such extrinsic impurities can affect the oxide-semiconductor interface and further complicate the physics of interface states. Hence, wherever possible, this discussion is on phenomena, experiments, and theories in which such extrinsic oxide ionic charges are negligible.

One can envision how the gross electronic properties of the oxide-semiconductor interface are manifested. One can imagine a perfect infinite semiconductor having a forbidden gap separating two bands of extended states called the valence and conduction bands. These states in which the carriers are characterized by a good quantum number (crystal momentum) are due to the long-range order in the crystalline semiconductor. However, to grow an oxide-semiconductor interface, one needs a surface. The introduction of a surface in the crystalline semiconductor breaks the long-range symmetry, with the subsequent result that electronic states localized near the surface can now exist in the gap. Carriers in these states cannot be characterized

¹N. J. Chou, *J. Electrochem. Soc.*, 118 (1971), 601.

*The elevated temperatures are used just to decrease the amount of time elapsed before a given amount of mobile ionic charge is transported to either interface.

by momentum alone since momentum is not a good quantum number. In Si, these states form two so-called surface bands centered slightly below and above the bulk conduction and valence bands. These bands were observed in work function and photoelectron threshold measurements on atomically clean Si surfaces.² Later, optical absorption due to transitions between these two bands was observed.³ Electron paramagnetic resonance studies have established that the surface valence band consists of unpaired electrons.⁴ Also, from photoemission studies, the surface valence band contains one electron per surface atom (8×10^{14} electrons cm^{-2}).^{5,6} Theoretical calculations by Appelbaum and Hamann show a "single band" of gap states that are highly localized in the surface and have an unmistakable dangling bond shape.⁷

Hence, these localized surface band states represent an unnatural state. Upon exposure to the atmosphere, the atomically clean surface undergoes chemical reactions by saturating most dangling bonds and, thus, reduces the surface-free energy. This reduction takes place via the chemical absorption of a layer of O_2 . The photoemission peak of the former surface valence band is practically eliminated.⁵ What occurs is that the surface valence band and O_2 p-orbitals form the oxide valence band below the Si band. Now as the Si surface is continually oxidized, some Si diffuses into the SiO_2 , while, at the same time, O_2 diffuses into the bulk Si. This is just another example of a system's lowering its free energy by the entropy of mixing. This process is continued in the manufacture of MOSFET devices until an oxide layer of approximately 100 nm is formed.

²F. G. Allen and G. W. Gobeli, *Phys. Rev.*, 127 (1962), 150.

³G. Cluarotti et al, *Phys. Rev.*, B4 (1971), 3398.

⁴D. Haneman, *Phys. Rev.*, 176 (1968), 705.

⁵L. F. Wagner and W. E. Spicer, *Phys. Rev. Lett.*, 28 (1972), 1381.

⁶D. E. Eastman and W. D. Grobman, *Phys. Rev. Lett.*, 28 (1972), 1378.

⁷J. A. Appelbaum and D. R. Hamann, *Phys. Rev. Lett.*, 31 (1973), 106.

We point out in section 2 that the interface should extend over several lattice spacings and should be very disordered. This disorder should give rise to fluctuations. In fact, in the course of their investigations on MOS-type devices, Nicollian and Goetzberger noticed a dispersion of interface-state time constants in the depletion region of gate voltage.⁸

At the same time, it was demonstrated both theoretically and experimentally that the strong surface electric field associated with a semiconductor inversion layer is sufficient to quantize motion of the charge carriers normal to the surface.⁹ The levels in the inversion region consist of electric subbands, each of which is a two-dimensional Block state associated with one of the quantized levels. Indeed, these conclusions were corroborated by electron-tunneling, capacitance, and far-infrared cyclotron resonance studies of the quantized levels.¹⁰

It was suggested further that electrons in these inversion layers also behave like electrons in a two-dimensional disordered system, the disorder being due to the random fluctuating interface potential independently proposed by Nicollian and Goetzberger.⁸ In other words, the random fluctuating potential should yield the characteristic temperature dependence of amorphous conductivity in the conductance channel, $\sigma \propto T^{1/(d+1)}$ at low temperatures, where d is the dimensionality of the system.¹¹ Indeed, such a dependence of the low-temperature

⁸E. H. Nicollian and A. Goetzberger, *Bell Syst. Tech. J.*, 45 (1967), 1055.

⁹F. Stern and W. E. Howard, *Phys. Rev.*, 163 (1967), 816; A. B. Fowler, F. F. Fang, W. E. Howard, and P. J. Stiles, *Phys. Rev. Lett.*, 16 (1966), 901.

¹⁰D. C. Tsui, *Phys. Rev.*, B4 (1971), 4438; *Phys. Rev.*, B8 (1973), 2657; S. James Allen, D. C. Tsui, and J. V. Dalton, *Phys. Rev. Lett.*, 32 (1974), 107; D. C. Tsui, G. Kaminsky, and P. H. Schmidt, *Phys. Rev.*, B9 (1974), 3524.

¹¹R. Am Abram, *J. Phys. Chem.*, 6 (1973), L379; V. D. S. Shante, *Phys. Lett.*, 43A (1973), 249.

channel conductance has been recently seen and reported.¹² The fluctuating potential at the interface is necessary to explain the behavior of the inversion layer carrier mobility as a function of carrier concentration and temperature.¹³ Finally, measurements of the resonant absorption of photons due to transitions between the quantized levels show a distortion of the resonance line width that can be caused by a fluctuating surface potential.^{14,15}

Hence, these independent measurements strongly indicate that the surface potential at an oxide-semiconductor interface is not a smooth function, but is more akin to a random fluctuating potential somewhat similar to that observed in amorphous solids. We theorize that these fluctuations are the result of the loss of long-range order as the Si is "alloyed" with the oxide. This alloying tends to cause band-tail states extending into the gap in both the Si valence and conduction bands. These states we call "intrinsic" interface states, since they arise from the inherent disorder introduced by the alloying. Also, in the oxide are localized states that cannot communicate with the semiconductor, metal electrodes, or both. These states are notorious hole traps. We speculate that any holes trapped in these states increase the fluctuations and, in turn, increase the band-tail states or interface states. Such a theory accounts for the U-shaped, structureless, measured density of states curves.¹⁴ It accounts also for an approximately equal number of electron and hole states. On the other hand, models that depend on an isolated microscopic defect to account for the interface states are hard pressed to explain all the characteristics of the measured density of states.

¹²H. Ibach and J. E. Rowe, *Phys. Rev.*, B9 (1974), 1951.

¹³A. G. Revesz et al, *J. Phys. Chem. Solids*, 28 (1967), 197.

¹⁴R. Castagne and A. Vapaille, *Electronic Letters*, 6 (1970), 691.

¹⁵M. Kuhn and E. H. Nicollian, *J. Electrochem. Soc.*, 118 (1971), 370.

In section 3, we review the derivation of the admittance of an MOS capacitor with a distribution of localized states. Then we indicate how one can interpret these interface potential fluctuations via a macroscopic theory of Brews.¹⁶ These interface states can be measured by a variety of techniques, one of which we have specifically considered--the quasi-static capacitance voltage measurement (QSCV).¹⁷ We also indicate the necessary conditions of reversibility that must be satisfied in order to use the QSCV technique.

2. MICROSCOPIC THEORY

2.1 Intrinsic Interface States

The MOS system is quite complicated. The first complication is that the system is heterogeneous--that is, the properties of the system are origin dependent. Also, the electronic properties range from extended conduction in the metal to phonon-assisted tunneling through band-tail states in the oxide. Nonetheless, we should like to speculate using the knowledge of the physics of ordered and disordered systems on the properties at and near the oxide-semiconductor interface.

Ion backscatter studies indicate that this region is not sharp.¹⁸ Instead, the oxide appears to be stoichiometric up to the interface while having an ever increasing concentration of Si. This is to be physically expected from the entropy of mixing. During the

¹⁶J. R. Brews, *J. Appl. Phys.*, 43 (1972), 2306; 3451.

¹⁷C. N. Berglund, *IEEE Trans. Electron Devices*, ED-13 (1966), 701; M. Kuhn, *Solid-State Electron.*, 13 (1970), 873.

¹⁸W. K. Chu, E. Lugujjo, and J. W. Mayer, *Appl. Phys. Lett.*, 24 (1974), 105.

growth process, two materials, the Si and oxide thereof, are present and in contact at high temperatures. The total system at this elevated temperature can reduce its free energy by increasing the entropy due to mixing. Therefore, one should expect a large concentration of Si in the oxide at the interface. On the other hand, the Si being used to grow the oxide is already saturated with a large concentration of O_2 , since the Si crystals used in MOSFET devices are pulled from quartz crucibles.* Therefore rather than being a sharp mathematical plane separating two nonmixed solid phases, the interface appears to be more of an alloyed heterojunction--the excess Si and O_2 concentrations persisting into the oxide and semiconductor regions, respectively. The adage that nature abhors a singularity is the rule in this case. Nevertheless, a description of the junction as a "gradual heterojunction" is indeed simplified. Not only does the junction undergo a compositional gradient, but long-range order disappears, and the nearest-neighbor lattice constant changes. These physical changes, needless to say, have severe ramifications on the electrical properties of the system and, in particular, at the oxide-semiconductor junction.

One approach to the problem of an oxide-semiconductor junction is to investigate the nature of the density of states in a gradual gap heterojunction. Unfortunately, this problem has yet to be solved. However, it can be qualitatively modeled by an alloy in which the composition, x , is a function of direction. The subsequent alloy, $A_x B_{1-x}$, can then closely model a graded heterojunction by the appropriate choice of the spatial composition dependence as indicated in figure 3 for a Fermi type of compositional dependence,

$$x = [\exp(-\beta z) + 1]^{-1}.$$

*At the melt temperature, there is an equilibrium distribution of dissolved O_2 in Si. Most O_2 remains in the Si crystal structure as bound interstitial impurities. The interaction of this interstitial O_2 with a lattice vacancy gives rise to the infamous Si-A center with an electron trapping level 0.17 eV below the conduction band.

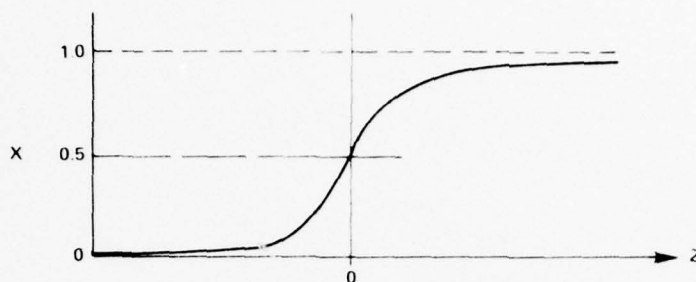


Figure 3. One possible dependence of composition of graded A_xB_{1-x} heterojunction.

Here, β is a measure of the amount of mixing, the "effective" junction width being just twice the inverse of β . From our knowledge of the alloy density of states for homogeneous materials,¹⁹ we can say that the density of states of a graded heterojunction should behave somewhat similarly to that in figure 4.²⁰ For simplicity, only one band has been shown. In the model, ϵ_A and ϵ_B are the mean band positions. As the concentration of the A species increases, an impurity band forms in which the states are purely localized as the hatched marks indicate (see fig. 4). This localized A band grows with increasing distance into the junction until, at $z = 0$, there are equal compositions of A and B. Then as the B species decreases, the A band becomes more and more extended until, at large distances, the material consists of all A atoms. This highly idealized picture serves two purposes: (1) the density of states is position dependent, and (2) there will exist *localized* states in and around the junction.

In our actual oxide-Si interface, the details are more complicated. The lattice constant changes, and the oxide is disordered (lacks long-range order). In the binary alloy model of a heterojunction, there is a basic lattice; the disorder originates in

¹⁹P. Soven, *Phys. Rev.*, 156 (1967), 809; B. Velicky, S. Kirkpatrick, and H. Ehrenreich, *Phys. Rev.*, 175 (1968), 746.

²⁰M. M. Sokoloski, *Bull. Am. Phys. Soc.*, 20 (1975), 426.

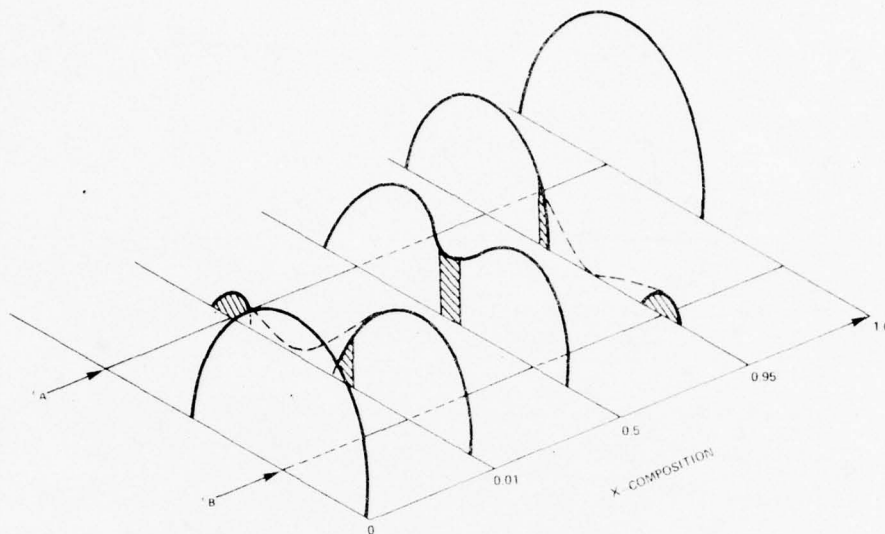


Figure 4. Possible dependence of density of states for alloy A_xB_{1-x} heterojunction: x has position dependence of fig. 3; point $x = 0$ corresponds to pure B material $z = -\infty$; while for $x = 1$, $z = +\infty$. For $x = 0.5$, $z = 0$, the middle of the heterojunction.

the random placement of A and B atoms on the lattice. This type of disorder is called compositional disorder. In the oxide-semiconductor case, there is also topological disorder. Here the oxide is not unlike that of an amorphous solid where the binding forces between the atoms are still similar to those in a crystal, but long-range order is absent while short-range order of a few lattice constants are generally present.²¹ From the angular dependence of the scattered radiation of an x-ray diffraction pattern, the radial or pair distribution function $4\pi r^2 \rho(r) dr$ can be obtained through a Fourier inversion. This yields the number of pairs of atoms separated by a distance lying between r and $r + dr$. As an example, the experimental radial distribution curves (RDC's) for amorphous and crystalline Si are shown in figure 5.²² If

²¹N. F. Mott and E. A. Davis, *Electronic Processes in Non-Crystalline Materials*, Clarendon Press, Oxford, England (1971).

²²S. C. Moss and J. F. Graczka, *Phys. Rev. Lett.*, **23** (1969), 1167; S. C. Moss and J. F. Graczka, *Proceedings of the 10th International Conference on the Physics of Semiconductors*, Cambridge, MA (1970), 658.

the peaks in the RDC are well separated from adjacent ones, then the area beneath the first peak, for instance, yields the number of atoms in the first coordination sphere; i.e., the first nearest neighbors in a crystal lie on the periphery of a sphere.

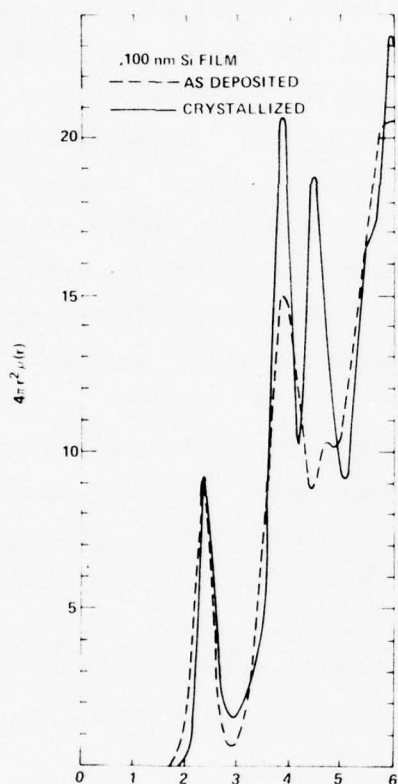


Figure 5. Radial distribution curves for amorphous and crystalline Si as determined from analysis of electron diffraction data.

For both the amorphous and crystalline states of Si, the first peak is at an interatomic spacing of 0.235 nm and has a coordination number of 4. Each atom is separated from four nearest neighbors by the lattice constant of 0.235 nm. The second peak is the same for both crystalline and amorphous Si with a spacing of 0.386 nm and coordination number of 12. However, the third peak present in the crystalline state is dramatically absent in the amorphous curve. This absence means that given a particular site, we no longer can predict with certainty the position of the third nearest neighbor atom. There

is loss of long-range order. This loss implies also that charge carriers can no longer be specified by a good quantum number of crystalline momentum. In actuality, the carrier's mobility is now a function of its energy.

Because of the loss of long-range order and associated fluctuations in matrix elements, the oxide gap cannot be described by the wide gap of an insulator. Electrons that make transitions out of the valence states into the conduction states do not necessarily leave behind holes with definite momentum or enter extended states. The loss of long-range order and presence of associated potential fluctuations lead to the possibility of extended and localized states as shown in figure 6. Now the density of states does not go to zero sharply at the valence or conduction band edge, but tails off. These band tails consist of localized states, i.e., states that conduct by phonon-assisted tunneling. Above a certain energy in the conduction band and below that in the valence band, the states are extended; transport can be considered as crystalline. This particular energy is known as the mobility edge and is designated as E_c and E_v in figure 7.

However, we have been discussing the loss of long-range order and potential fluctuations in homogeneous systems. In heterogeneous systems, the radial distribution function must now be origin dependent. For instance, if one examines the radial distribution function (RDF) in the bulk of the Si in our MOS-structure, one would obtain the crystalline RDC's. In contrast, if the RDF were examined in the oxide bulk, one would obtain RDC's similar to those of amorphous, glassy SiO_2 .

The oxide-semiconductor junction is not sharp. Also, there is a loss of long-range order and an associated increase in potential fluctuations as the origin is moved from the bulk Si to the oxide-semiconductor interface. Therefore, the interface should be characterized, in part, by a region of localized states that lie in the semiconductor gap. These states, indicated by the hatched areas in figures 4 and 6, would then be a manifestation of the loss of long-range order and an increase in potential fluctuations. These states would

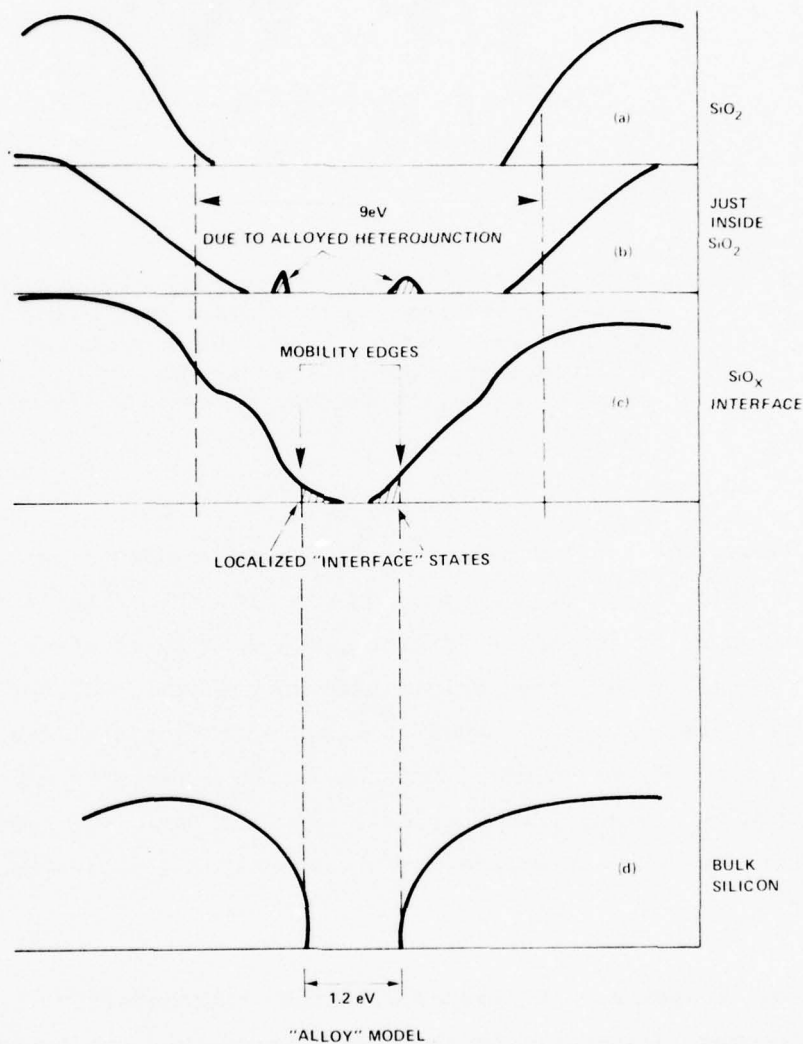


Figure 6. Metamorphosis of density of states from that in bulk SiO_2 (a) to that in bulk Si (d).

then be intrinsic interface states. Their sole claim to existence would be due to the glassy amorphous SiO_2 to crystalline Si transition, and they should occur in all such systems.

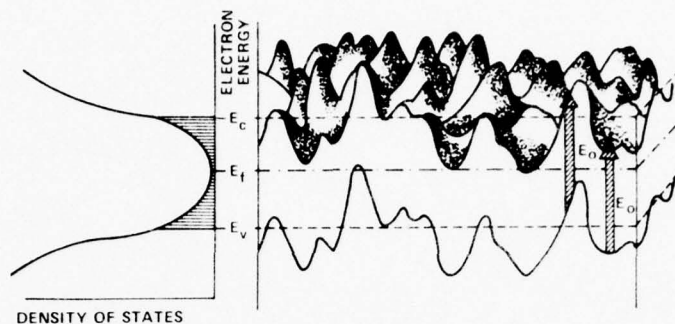


Figure 7. Heterogeneous model: right-hand side shows edges of valence and conduction bands modified by long-wavelength electrostatic potential fluctuations; optical transitions take place with energy E_o ; localized states lie between E_c and E_o .

Hence, one can formulate the following argument: As the origin is moved from the bulk semiconductor in the direction of the oxide-semiconductor interface (fig. 6), the density of states undergoes a metamorphosis. For the origin deep in the semiconductor bulk, the density of states is just equal to that of the crystalline material. The RDF is that of the ordered material. The effects of the interface are screened out by any free carriers. As the origin is moved closer and closer to the interface, the effects of disorder become more important.

For instance, in figure 8, the tetrahedrally coordinated lattice becomes disordered as the origin approaches the interface. At sites labeled 2 and 3, the number of semiconductor atoms in the first coordination sphere begins to differ from that in the bulk semiconductor. Close to the interface, this loss of long-range order

introduces localized states in the Si energy gap as indicated in figure 6. These localized states are in "communication" with the bulk semiconductor; i.e., there can be transport in and out of these states to the bulk semiconductor valence and conduction bands.

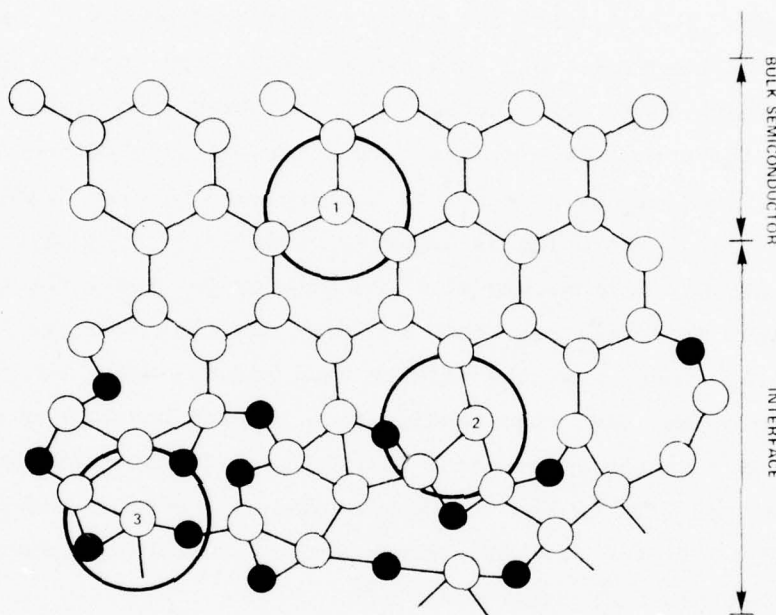


Figure 8. Transition from glassy amorphous SiO_2 to crystalline Si state.

There is an approximately equal number of these states above and below the intrinsic Fermi level as can be seen from figure 7. This U-shape for the localized states, more popularly known as interface states, has been seen experimentally by a whole host of independent experimenters.^{14,23}

Previous theories of these states have accounted for the shape of the interface-state density curves as being due to a particular defect at the interface. However, it is exceedingly difficult to justify that

¹⁴R. Castagne and A. Vapaille, *Electronic Letters*, 6 (1970), 691.

²³R. Castagne and A. Vapaille, *Surface Science*, 28 (1971), 157; *Electron. Lett.* 6 (1970), 691; D. J. Silversmith, *J. Electrochem. Soc.*, 119 (1972), 1589.

this level spreads across the gap (for Si, energies exceed 1 eV) because a level splits as a result of interactions with the immediate environment. Also, it is difficult to make isolated defect trap holes and then electrons depending on the position of the Fermi level. Therefore, the result of alloying the semiconductor with its oxide introduces the loss of long-range order and potential fluctuations. These result in a distribution of localized gap states referred to as band tails or interface states. In tetrahedrally bonded semiconductors, because of alloying, remnants of the s-p bonding and antibonding bands persist into the oxide as impurity bands (fig. 4, 6(b)). These states may or may not communicate with the bulk oxide; i.e., the phonon-assisted tunneling probabilities may be very small. Some of these states, especially those near the valence band edges, may be responsible for trapping holes and thus leading to a trapped positive charge density in the oxide. On the other hand, it is expected that transport in the oxide can be modeled by the continuous-time-random-walk model of Scher and Montroll modified by an imperfectly absorbing boundary at the oxide-semiconductor interface.^{24, 25}

2.2 Extrinsic Interface States

Experimentally, it is well known that oxide charge is trapped close to the interface and ordinarily cannot tunnel into the bulk semiconductor. This trapping may result from a persistent impurity band extending into the oxide due to the incomplete alloying at the interface (a preponderance of Si atoms, for instance). The trapping should give rise to an electrostatic potential. However, because of the inherent disorder in the interface, this charge and its resultant

²⁴H. Scher and E. W. Montroll, *Phys. Rev.*, B12 (1975), 2455; H. E. Boesch, F. B. McLean, J. M. McGarrity, and G. A. Ausman, Jr., *IEEE Trans. Nucl. Sci.*, NS-22 (1975), 2163.

²⁵F. B. McLean, G. A. Ausman, H. E. Boesch, J. M. McGarrity, J. *Appl. Phys.*, 47 (1976), 1529.

potential are not uniform, but fluctuate about some mean. These fluctuations, in turn, produce further fluctuations that cause the bands to vary as schematically indicated in figure 7. Hence, these potential fluctuations (as compared to potential fluctuations due to matrix elements fluctuating about some mean value) also lead to trapping states and band tails. Therefore, the interface-state density also is a function of the amount of charge trapped in the oxide; i.e., the more charge trapped in the oxide, the greater the potential fluctuations and the more the interface-state density.

One can then define those states due to potential fluctuations from a trapped oxide charge distribution as being "extrinsic." Therefore, the overall microscopic picture is that the intrinsic interface states are inherently due to the loss of long-range order due to the nature of the oxide-semiconductor heterojunction. Also, charges trapped in localized oxide states, which may be due to remanant s-p bonding and antibonding states of the semiconductor, can cause an increase in the density of interface states, and these new states are extrinsic. Extrinsic states are due also to impurities and defects at the interface not accounted for in the heterojunction model.

3. FORMULATION

3.1 Admittance for Distribution of Interface States

The admittance of a distribution of localized states in the semiconductor forbidden gap and fluctuations in the interface potential can be derived by (1) calculating the admittance of a single localized level via Shockley-Read statistics,²⁶ (2) averaging over a density of localized states, and (3) averaging over fluctuations in interface potential.⁸

⁸E. H. Nicollian and A. Goetzberger, *Bell Syst. Tech. J.*, 45 (1967), 1055.

²⁶W. Shockley and W. T. Read, *Phys. Rev.*, 87 (1952), 835.

States that occur in the gap are bound states. The capture rate of electrons taken as the majority carrier at some energy is then

$$R_n(t) = N_s c_n [1 - f(t)] n_s(t), \quad (1)$$

while the emission rate is

$$G_n(t) = N_s e_n f(t), \quad (2a)$$

where N_s is the density of bound interface states per cm^{-2} , c_n is the electron capture probability in cm^3/s , e_n is the electron emission constant in s^{-1} , $f(t)$ is the Fermi distribution at time t , and $n_s(t)$ is the electron density at the localized trap site at time t in cm^{-3} . This is a special case in which the density of interface states (in $\text{cm}^{-2} \text{eV}^{-1}$) is given by

$$N_{ss}(\psi) = N_s \delta(\psi - \psi_t),$$

where ψ_t is the energy of the bound state. Since electrons are being trapped, the bound states at the interface are either negatively charged (the state is filled) or neutral (the state is unoccupied). Such an interface state is sometimes called an acceptor surface state. Then the trap occupation probability

$$f_o(t) = [1 + \exp(\psi_t - \psi_F(t))/kT]^{-1} = [1 + \exp(\psi_t - \psi_B + \psi_s(t))/kT]^{-1} \quad (2b)$$

where $\psi_F(t)$ is the Fermi level, ψ_B is the bulk Fermi level, and ψ_s is the surface potential. In equation (1), the capture rate depends on the occupancy of the bound state, i.e., $N_s(1 - f(t))$, and the number of electrons, $n(t)$, that are available to make a transition to this bound state. On the other hand, the transition from a bound state to the conduction-band continuum is independent of the final-state Fermi

function only in depletion. Hence, equation (2a) is a good approximation, except in heavy inversion or accumulation. The net current flowing equals the electronic charge, q , multiplying the difference of the capture and emission rates, namely,

$$i_s(t) = qN_s c_n [1 - f(t)] n_s(t) - qe_n N_s f(t) . \quad (3)$$

For no external alternating stimulus, $i_s(\text{dc}) = 0$. This is sometimes referred to as detailed balancing. Equation (3) can be solved in a linear approximation by expanding all time-dependent variables, $x(t)$, in a Taylor series expansion about their static values,

$$\begin{aligned} x(t) &= x_o + \left. \partial x / \partial t \right|_0 \delta t + \dots \\ &= x_o + \delta x . \end{aligned} \quad (4)$$

These are substituted into the current equation, i.e.,

$$\begin{aligned} i_s(t) &= qN_s c_n [(1 - f_o)n_{so} + (1 - f_o)\delta n_s - n_{so}\delta f] \\ &\quad - qe_n N_s (f_o + \delta f) , \end{aligned} \quad (5)$$

where second-order terms have been neglected. Equation (5) can be manipulated so that

$$\begin{aligned} qN_s c_n (1 - f_o)n_{so} - qe_n N_s f_o &= i_s(t) - qN_s c_n [(1 - f_o)\delta n_s - n_{so}\delta f] \\ &\quad + qe_n N_s \delta f . \end{aligned} \quad (6)$$

The left-hand side is independent of the time and, thus, is a constant. From detail balancing, this constant is set equal to zero. Statically, no net current flows--a particle emitted from the bound state is then captured. This places a constraint on the emission rate, namely,

$$e_n = c_n n_{so} (1 - f_o) / f_o . \quad (7)$$

This can be substituted into the right-hand side of equation (6), and an expression for the current is obtained:

$$\begin{aligned} i_s(t) &= qN_s c_n \left[(1 - f_o) \delta n_s - n_{so} \frac{\delta f}{f} \right] \\ &= qN_{ss} \frac{df}{dt} . \end{aligned} \quad (8)$$

Hence, for an applied field with frequency ω ,

$$\begin{aligned} \frac{df}{dt} &= i\omega \delta f \\ &= c_n (1 - f_o) \delta n_s - c_n n_{so} \frac{\delta f}{f} . \end{aligned} \quad (9)$$

This can be subsequently solved for δf .

$$\begin{aligned} \delta f &= \frac{f_o c_n (1 - f_o) \delta n_s}{c_n n_{so} + i\omega f_o} \\ &= \frac{f_o (1 - f_o)}{1 + i\omega f_o / c_n n_{so}} \frac{\delta n_{so}}{n_{so}} . \end{aligned} \quad (10)$$

The substitution of equations (9) and (10) into equation (8) yields

$$i_s(t) = \frac{i\omega q N_s f_o (1 - f_o)}{1 + i\omega f_o / c_n n_{so}} \frac{\delta n_{so}}{n_{so}} . \quad (11)$$

From

$$n_s = n_i \exp (u_s - u_B) , \quad (12)$$

it can be shown that

$$\begin{aligned} \delta n_s &= n_i \exp (u_s - u_B) \delta u_s \\ &= n_s \delta u_s , \end{aligned} \quad (13)$$

where u_s and u_b are the interface and bulk potentials in units of kT/q and n_i is the intrinsic carrier density.⁸ Therefore,

$$\frac{\delta n_s}{n_{so}} = \delta u_s \quad (14)$$

$$= q/kT \times \delta \psi_s, \quad (15)$$

where ψ_s is the interface potential in electron volts. Therefore, the substitution of equation (14) into equation (11) finally yields an expression for the admittance of a single bound state N_s , i.e.,

$$i_s(t) = Y_s(\omega) \delta \psi_s, \quad (16)$$

where

$$Y_s(\omega) = i\omega \frac{q^2 N_{so} f_o (1 - f_o)}{kT (1 + i\omega f_o / c n_{so})}. \quad (17)$$

Now if one calls

$$C_{ss}^0 \equiv q^2 N_{so} f_o (1 - f_o) / kT \quad (18)$$

and defines a majority carrier time constant

$$\tau \equiv f_o / c n_{so}, \quad (19)$$

then one can write

$$Y_s(\omega) = G_p(\omega) + i\omega C_p(\omega), \quad (20)$$

where the equivalent capacitance and parallel conductance are given as

$$C_p = \frac{C_{ss}^0}{1 + \omega^2 \tau^2} \quad (21)$$

⁸E. H. Nicollian and A. Goetzberger, *Bell Syst. Tech. J.*, 45 (1967), 1055.

and

$$G_P = \frac{C_{ss}^0 \omega^2 \tau^2}{1 + \omega^2 \tau^2} . \quad (22)$$

The dc or static limit of the equivalent capacitance is just C_{ss}^0 . Also, $f^0(1 - f^0)$ is sharply peaked with spread kT about the bound state energy, ψ_t . There, C_{ss}^0 has its maximum value when $\psi_t = \psi_f$. For the MOS capacitor, this equivalent capacitance appears in parallel with the space-charge capacitance, shown as follows.

The total charge density for a given interface potential is

$$Q_T = Q_{sc} + Q_s + Q_f , \quad (23)$$

where Q_{sc} is the charge in the Si-space-charge region, Q_s is the charge in the interface (bound) states, and Q_f is the charge in the fixed states. The charge in the fixed states, as the name implies, cannot communicate with either the metal or the semiconductor electrodes. "Communicate" means to make a quantum mechanical transition via some process such as tunneling or phonon-assisted hopping from the bound-state site (in the oxide) to either the metal or the semiconductor. The total current is then the time rate of change of the total charge,

$$i_s(t) = \frac{dQ_{sc}}{dt} + \frac{dQ_s}{dt} \quad (24a)$$

$$= \frac{dQ_{sc}}{d\psi_s} \frac{d\psi_s}{dt} + i_s(t) , \quad (24b)$$

$$i_s(t) = (i\omega C_p + Y_s) \delta\psi_s . \quad (24c)$$

Equation (24c) is derived partly from the substitution of equation (16) for the bound-state current and the realization that

$$C_{sc} = dQ_{sc} / d\psi_s \text{ and } \psi_s = \psi_{so} + \delta\psi_{so}$$

$$\text{where } \delta\psi_{so} = a \exp(i\omega t) .$$

Hence, equation (24c) shows that the bound-state admittance appears in parallel with the capacitance of the semiconductor space-charge layer. Figure 9 shows the equivalent circuit for the MOS capacitor with discrete noninteracting bound states that are physically in the oxide-semiconductor region.

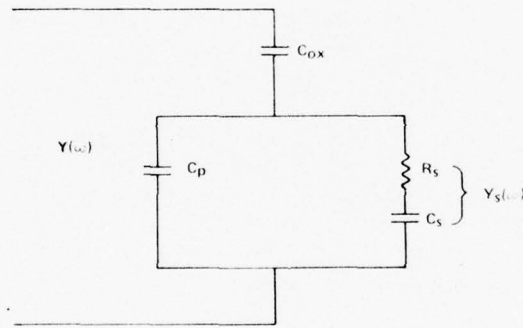


Figure 9. Circuit for metal-oxide-semiconductor capacitor with discrete noninteracting bound states in insulator-semiconductor interface.

The admittance due to a number of noninteracting bound states is given by equation (17). This can be easily extended to a distribution of localized-interface states by integrating over the potential, since N_{ss} is now a function of potential, i.e.,

$$Y_{ss}(\omega) = i\omega \left(\frac{q^2}{kT} \right) \int \frac{N_{ss}(\psi) f_o (1 - f_o) d\psi}{1 + i\omega f_o / c_{nso}}, \quad (25)$$

where $N_{ss}(\psi)$ is the density of states and ψ is energy.²⁵ The Fermi distribution is now a continuous function of potential (i.e., ψ_t is now a continuum of values, ψ).

For a density-of-states function and a capture cross section that do not change appreciably within kT of ψ_f , the distribution, $N_{ss}(\psi)$, can be taken out of the integral and evaluated at $\psi_f = \psi_s - \psi_B$, and the capture cross section can be treated as constant. Then one can make the substitution that

$$df_o/d\psi = -q/kT \times f_o(1 - f_o)$$

and transform equation (25) into an integral over f_o with lower and upper boundaries of 0 and 1, respectively. The integrand is separated into real and imaginary parts,

$$\int = \int_0^1 \frac{df_o}{1 + f_o^2 \omega^2 \tau^2} - i\omega\tau \int_0^1 \frac{f_o df_o}{1 + f_o^2 \omega^2 \tau^2} \quad (26a)$$

This can be readily integrated to yield

$$Y_{ss} = \frac{qN_{ss}}{2\tau} \ln(1 + \omega^2 \tau^2) + iq \frac{N_{ss}}{\tau} \tan^{-1}(\omega\tau) \quad (26b)$$

The corresponding conductance and admittance are given by

$$G_{ss}(\psi_s) = \frac{qN_{ss}(\psi_s)}{2\tau} \ln(1 + \omega^2 \tau^2) \quad (27a)$$

and

$$C_{ss}(\psi_s) = qN_{ss}(\psi_s) \frac{1}{\omega\tau} \tan^{-1}(\omega\tau) \quad (27b)$$

²⁵F. B. McLean, G. A. Ausman, H. E. Boesch, J. M. McGarrity, J. Appl. Phys., 47 (1976), 1529.

Equations (27a) and (27b) yield the proper static equation $\phi = 0$; in particular, the static capacitance due to a distribution of surface states is

$$C_{ss}(\psi_s) = qN_{ss}(\psi_s) . \quad (28)$$

This equation could have been derived in a more straightforward manner by integrating the expression for the dc or static capacitance for the case of (noninteracting) isolated bound states,

$$C_{ss}(\psi_s) = \int C_{ss}^0(\psi) d\psi \quad (29a)$$

$$= \int q^2 N_{ss}(\psi) f_o(1 - f_o) / kT d\psi , \quad (29b)$$

in which $N_{ss}(\psi)$ does not vary much over energy.

3.2 Fluctuations in Potential

To treat the problem of fluctuating interface potentials, we shall employ the phenomenological approach of Nicollian and Goetzberger⁸ as extended by Brews.¹⁶ According to Brews,¹⁶ the interface charge due to any trapped oxide charge and charge trapped in the Si-band-tail states near the interface can be treated by a distribution of uncorrelated characteristic areas, α , each with a charge density as shown in figure 10. Each characteristic area varies in properties from other areas according to some probability distribution. For each of the characteristic areas, one can write

$$(\psi_g - \psi_s) C_{ox}^\alpha = Q^\alpha + Q_{sc}^\alpha(\psi_s) , \quad (30)$$

⁸E. H. Nicollian and A. Goetzberger, *Bell Syst. Tech. J.*, 45 (1967), 1055.

¹⁶J. R. Brews, *J. Appl. Phys.*, 43 (1972), 2306; 3451.

where ψ_g and ψ_s are the gate and surface potentials, respectively, of the α th area. Also, C_{ox}^α , Q^α , and Q_{sc}^α are the oxide capacitance, charge, and space charge associated with area α . According to Brews,¹⁶ a similar expression is assumed to be valid for the entire macroscopic structure,

$$(\psi_g - \bar{\psi}_s)C_{ox} = \bar{Q} + \bar{Q}_{sc}(\psi_s) . \quad (31)$$

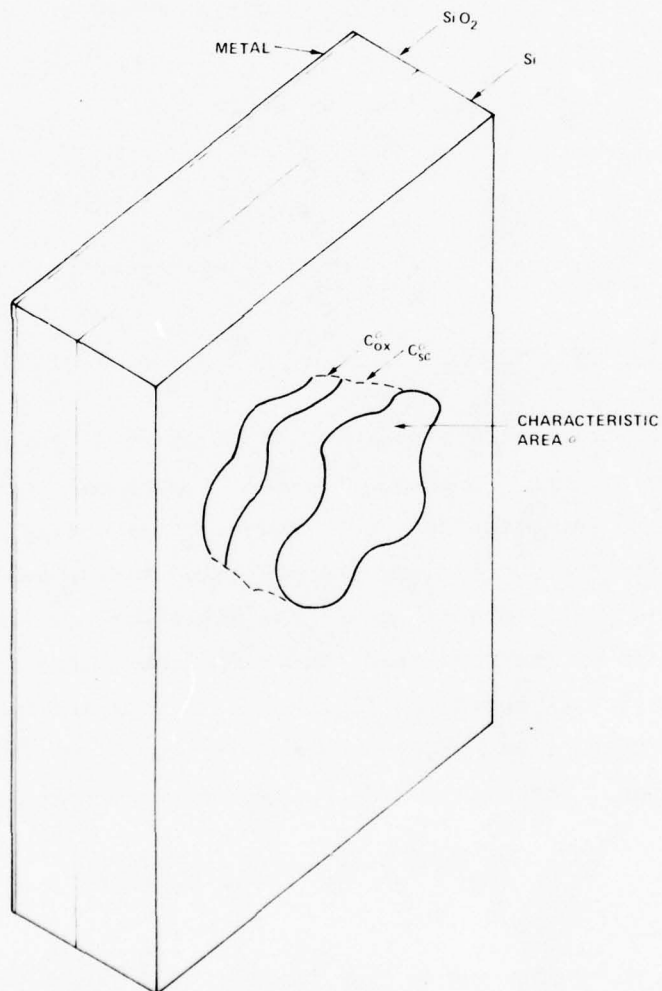


Figure 10. Metal-oxide-semiconductor structure divided into two arbitrarily small areas of uniform charge density.

¹⁶J. R. Brews, *J. Appl. Phys.*, **43** (1972), 2306; 3451.

The bars indicate that the quantities that are statistically varying over the macroscopic structure have been suitably averaged. What we really seek is the average of not the macroscopic structure, but the α th area. It can be found by dividing equation (31) by $N = (\alpha/A)^{-1}$, where N is the number of macroscopic areas, while A is the total area of the macroscopic structure. Then equation (31) becomes

$$(\psi_g - \bar{\psi}_s) C_{ox}^\alpha = \bar{Q}^\alpha + \overline{Q_{sc}^\alpha(\psi_s)} . \quad (32)$$

In the Brews^{8,16} approach, C_{ox} is statistically a constant. The bars with superscript α 's indicate averages of the parameters describing the α th area.

The derivations of the true values must be found about their average values. Hence, equation (32) is subtracted from equation (31) to yield

$$(\psi_s - \bar{\psi}_s) C_{ox}^\alpha = \bar{Q}^\alpha - \bar{Q}^\alpha + \left[\overline{Q_{sc}^\alpha(\psi_s)} - \overline{Q_{sc}^\alpha(\bar{\psi}_s)} \right] . \quad (33)$$

Unfortunately, the space charge is a nonlinear function of the surface potential. However, for small surface potential fluctuations, the average space charge can be linearized as follows:

$$\overline{Q_{sc}^\alpha(\psi_s)} \approx \bar{\psi}_s C_{sc}^\alpha(\bar{\psi}_s) . \quad (34)$$

⁸E. H. Nicollian and A. Goetzberger, *Bell Syst. Tech. J.*, 45 (1967), 1055.

¹⁶J. R. Brews, *J. Appl. Phys.*, 43 (1972), 2306; 3451.

The total charge on each area consists of fixed charges that are not in communication with either the metal or the semiconductor electrode or charges in states that are mobile, i.e., interface states,

$$Q^\alpha - \overline{Q^\alpha} = Q_f^\alpha - \overline{Q_f^\alpha} + Q_{ss}^\alpha - \overline{Q_{ss}^\alpha}.$$

A crucial assumption of Brews¹⁶ is that since the interface charge, Q_{ss}^α , is mobile, these charges, on one hand, tend to screen out potential fluctuations and, on the other hand, tend to increase the potential fluctuations by trapping additional charges. Hence, this assumption can be modeled in a quasi-self-consistent manner by decomposing the interface charge into two components,

$$Q_{ss}^\alpha - \overline{Q_{ss}^\alpha} = C_{ss}^\alpha (\psi_s - \overline{\psi_s}) + \delta Q_{ss}^\alpha, \quad (36)$$

where the first term accounts for the screening and the last accounts for inhomogeneities. Then, following Brews,¹⁶ we define the variation in fixed charge by

$$\delta Q_f^\alpha \equiv Q_f^\alpha - \overline{Q_f^\alpha} \quad (37)$$

and find that the variation in total interface charge can be written as

$$\delta Q^\alpha \equiv \delta Q_f^\alpha + \delta Q_{ss}^\alpha. \quad (38)$$

By the substitution of equations (33) to (37) into equation (38), one finally obtains the variations (fluctuations) in the interface charge in terms of the variations (fluctuations) in the surface potential as

$$\delta Q^\alpha = [C_{ox}^\alpha + C_{ss}^\alpha (\overline{\psi_s}) + C_{sc}^\alpha (\overline{\psi_s})] \delta \psi_s. \quad (39)$$

¹⁶J. R. Brews, *J. Appl. Phys.*, 43 (1972), 2306; 3451.

Hence,

$$\overline{(\delta\psi_s)^2} = \left[C_{ox}^\alpha + C_{ss}^\alpha(\psi_s) + C_{sc}^\alpha(\psi_s) \right]^{-2} (\delta Q^\alpha)^2. \quad (40)$$

However,

$$\overline{(\delta Q^\alpha)^2} = \overline{(\delta Q_f^\alpha)^2} + \overline{(\delta Q_{ss}^\alpha)^2} + 2 \overline{(\delta Q_f^\alpha)(\delta Q_s^\alpha)}. \quad (41)$$

In the approach of Nicollian and Goetzberger,⁸ the last cross term in equation (41) is neglected, since the two charge distributions are considered uncorrelated, and the term $C_{ss}^\alpha(\psi_s)$ is absent in equation (40). If one defines capacitance per unit area by dividing by α , i.e., $C_{ox} = \alpha^{-1} C_{ox}^\alpha$, then

$$\sigma(\psi_s) = \frac{W(\psi_s)}{W(\psi_s) [C_{ox} + C_{ss}(\psi_s)] + \epsilon_{si}} \left(\frac{qQ}{\alpha} \right)^2 \quad (42)$$

where $W(\psi_s)$ is the space charge width shown in figure 11, ϵ_{si} is the dielectric constant of Si, and q is the electronic charge. As is pointed out by Brews,¹⁶ a large C_{ss} leads to a smaller σ^2 , which is a result of the screening effect.

3.3 Inclusion of Interface Potential Fluctuations on Admittance

From accumulation to flat band, the majority carriers in the semiconductors tend to screen and damp out fluctuations in the interface potential as can be seen from equation (42). However, from flat band to depletion, the screening effect is drastically decreased while more image charge appears in the metal electrode and causes fluctuations. The effects of the fluctuations should increase with increasing depletion width saturating at inversion. In contrast,

⁸E. H. Nicollian and A. Goetzberger, *Bell Syst. Tech. J.*, **45** (1967), 1055.

¹⁶J. R. Brews, *J. Appl. Phys.*, **43** (1972), 2306; 3451.

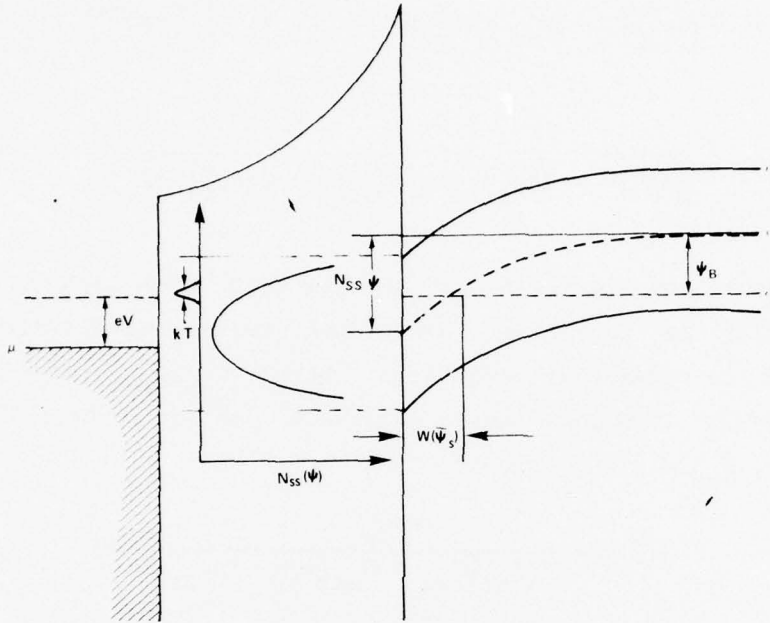


Figure 11. Oxide-semiconductor interface.

surface states oppose any increases in interface potential fluctuations by filling and unfilling, to compensate for variations in the mean trapped and interface charges. The zero frequency (quasi-static) surface-state capacitance averaged over the fluctuations in the interface potential is given by

$$\overline{C_{ss}(\psi)} = \frac{C_M(\psi)C_{ox}}{C_{ox} - C_M(\psi)} - \overline{C_{sc}(\psi)}, \quad (43)$$

where $C_M(\psi)$ is the measured value of the capacitance, C_{ox} is the geometric capacitance of the oxide layer, and $\overline{C_{sc}}$ is the average space-charging capacitance. The static or zero frequency average surface-state capacitance can be written as

$$\overline{C_{ss}(\psi_s)} = \int qN_{ss}(\psi) P(\psi, \bar{\psi}_s) d\psi_s, \quad (44)$$

where the kernel is given as

$$P(\psi, \bar{\psi}_s) = (2\pi\sigma^2)^{-1/2} \exp \left[-(\psi - \bar{\psi}_s)^2 / \sigma^2(\bar{\psi}_s) \right]. \quad (45)$$

Hence, $N_{ss}(\psi)$ is the density of interface-states function being nonzero only for $\bar{\psi}_s$ falling in the energy interval between the Si conduction and valence bands. It is also a positive definite compact function whose area yields the total number of interface states. The variance, $\sigma^2(\bar{\psi}_s)$, is given by equation (42). For a p-type semiconductor, the space-charge width is given approximately by

$$W(\bar{\psi}_s) = 0, \quad \bar{\psi}_s < \psi_{FB} \quad (46a)$$

$$= \left(\frac{2\epsilon_{si}\bar{\psi}_s}{qN_A} \right)^{1/2} \psi_{FB} \leq \bar{\psi}_s \leq \psi_{INV} \quad (46b)$$

$$= \left(\frac{2\epsilon_{si}\psi_{INV}}{qN_A} \right)^{1/2} \psi_{INV} \leq \bar{\psi}_s, \quad (46c)$$

where ψ_{FB} is the flat-band potential, N_A is the acceptor density, and ψ_{INV} is the inversion value of the interface potential,

$$\psi_{INV} = \frac{2kT}{q} \ln (N_A/n_i), \quad (47)$$

where n_i is the intrinsic carrier concentration at temperature T . Therefore, the functional dependence of all quantities on the surface potential is known. Hence, in accumulation, where most of the carriers are heavily screening the interface potential fluctuations, the space charge width is approximately zero. In this region, the fluctuations are ineffective, i.e.,

$$P(\psi, \bar{\psi}_s) = \delta(\psi - \bar{\psi}_s), \quad (48)$$

where $\delta(\psi - \bar{\psi}_s)$ is the dirac delta function. From flat band to inversion, the variance becomes a monotonically increasing function of space-charge width. The bar is dropped from $\bar{\psi}_s$ for notational simplicity.

The corresponding damping effect of the fluctuating potential by the surface states manifests itself in the dependence of the variance on the true surface-state capacitance, i.e.,

$$C_{ss}(\psi) = qN_{ss}(\psi) . \quad (49)$$

To determine $N_{ss}(\psi)$, the basic equation to be solved is

$$C_p(\psi_s) = \frac{C_M(\psi_s)C_{ox}}{C_{ox} - C_M(\psi_s)} \quad (50)$$

$$= \int_{\psi_v}^{\psi_c} [qN_{ss}(\psi) - C_{sc}(\psi)] P(\psi, \psi_s) d\psi , \quad (51)$$

where ψ_c and ψ_v are the interface potentials at the conduction and valence band edges, respectively. Equation (51) must be solved self-consistently, since $P(\psi, \psi_s)$, in turn, is a function of $N_{ss}(\psi)$. $C_p(\psi_s)$ is the parallel capacitance value of the surface state and space-charge capacitance. The gap, $\psi_c - \psi_v$, is divided into N parts of equal width, $\Delta\psi$. Then the first order in $\Delta\psi$, equation (51), can be written as

$$C_p(\psi_s) = \sum_{i,j=1}^{N+1} [qN_{ss}(\psi_i) - C_{ss}(\psi_i)] P(\psi_i, \psi_s) \Delta\psi , \quad (52)$$

where

$$\psi_1 = \psi_v \quad \text{and} \quad \psi_{N+1} = \psi_c .$$

Also, ψ_s can be divided into N units. Then

$$C_p(\psi_{sj}) = \sum_{i,j=1}^{N+1} \left[qN_{ss}(\psi_i) - C_{sc}(\psi_i) \right] P(\psi_i, \psi_{sj}) \Delta\psi . \quad (53)$$

Then one can define the following N -fold vectors

$$C_p \equiv \frac{1}{\Delta\psi} \left[C_p(\psi_{sj}) \right] , \quad (54a)$$

$$qN_{ss} = \left[qN_{ss}(\psi_i) \right] , \quad (54b)$$

$$C_{ss} = \left[C_{ss}(\psi_i) \right] , \quad (54c)$$

and the square matrix

$$P = \left[P(\psi_i, \psi_{sj}) \right] . \quad (55)$$

Then equation (52) can be simply written as

$$C_p = \left[qN_{ss} - C_{sc} \right] P(N_{ss}) , \quad (56)$$

where the dependence of P on N_{ss} has been shown. For P nonsingular, one can write

$$qN_{ss} = P(N_{ss})^{-1} C_p + C_{sc} . \quad (57)$$

If one defines the initial value $N_{ss}^0 \equiv \langle N_{ss} \rangle$ as the average measured value, then one can iteratively solve for N_{ss} , i.e.,

$$qN_{ss}^{i+1} = P^{-1}(N_{ss}^i)^{-1} C_p + C_{sc} . \quad (58)$$

4. QUASI-STATIC CAPACITANCE VOLTAGE METHOD FOR MEASUREMENT OF DENSITY OF INTERFACE STATES

4.1 Criteria for Reversibility

Three common experimental techniques are used to determine the density of interface states at a heterojunction such as that found in an MOS capacitor. These are the Gray-Brown,²⁷ Nicollian-Goetzberger,⁸ and QSCV²⁸ techniques.

In the Gray-Brown technique,²⁷ the variation in the charge density bound in the interface states is measured after the bulk Fermi level is displaced by a temperature change in the device. The Gray-Brown technique has been shown to be invalid at large interface-state densities, e.g., $10^{13} \text{ cm}^2 (\text{eV})^{-1}$.²⁹ These temperature-dependent techniques and variations thereof give rise to a peak in the density of interface states near each of the Si conduction and valence band edges. These peaks are highly suspect, since they have not been seen by any other experimental technique.

In the Nicollian-Goetzberger⁸ conductance technique, the measurements are limited in the accumulation end of the range, because the capture cross section is difficult to measure, and the interface density of the states is rapidly varying over several kT. Hence, the density of interface states is obtained in a limited region bound by the value of the surface potential corresponding to mid gap and flat band.

⁸E. H. Nicollian and A. Goetzberger, *Bell Syst. Tech. J.*, 45 (1967), 1055.

²⁷P. V. Gray and D. M. Brown, *Appl. Phys. Lett.*, 8 (1966), 31;
D. M. Brown and P. V. Gray, *J. Electrochem. Soc.*, 115 (1968), 760.

²⁸G. Dedherck, R. Van Overstraeten, and G. Brown, *Solid-State Electron.*, 16 (1973), 1451.

²⁹H. A. Mar and J. Simon, *Solid-State Electron.*, 17 (1974), 131.

³⁰M. Kuhn, *Solid-State Electron.*, 13 (1970), 873.

In the QSCV technique,²⁸ the interface potential is varied so that the system is always at equilibrium. Small errors in the integration constant have a great influence on the density of states value in accumulation and strong inversion. Nevertheless, it is superior to low frequency capacitance-voltage techniques when the minority carrier lifetimes are large, since in these instances, the generation recombination times are very small.³⁰

The advantage in the use of the QSCV technique²⁸ is that the system at all times is at thermodynamic equilibrium. Hence, the capacitance of the MOS system is just the oxide capacitance in series with a parallel combination of the average space-charge and interface-state capacitances for each value of the interface potential (gate potential) as given by equation (43). In other words, parameters dependent on the charge-carrier lifetimes and appearing as resistive components are zero for a static measurement. The QSCV technique involves sweeping the interface potential, ψ_s , at a certain rate. The criteria for thermodynamic reversibility, closely following the work of Kuhn,³⁰ is that

$$\tau_j (d\psi_B/dt) \leq kT/q, \quad (59)$$

for j corresponding to either electrons or holes. The lifetime τ_j is given by

$$\tau_j = (\bar{v}\sigma_j n_i)^{-1} \exp \left[\frac{q(\psi_B - \psi_s)}{kT} \right], \quad (60)$$

where \bar{v} is the average drift velocity and σ_j is the capture cross section due to the interface states for either electrons or holes.

²⁸G. Dedherck, R. Van Overstraeten, and G. Brown, *Solid-State Electron.*, 16 (1973), 1451.

³⁰M. Kuhn, *Solid-State Electron.*, 13 (1970), 873.

Hence, equation (59) states that the interface potential sweep rate must be such that the carriers making transitions in and out of the interface states can follow the changing potential at temperature T . If so, then the system at this sweep rate is always in equilibrium. In addition, in inversion, the sweep rate must be less than the minority-carrier generation rate. However, in the QSCV technique, the longest time constant is about 10^{-2} s at room temperature, which is much smaller than the minority-carrier generation rate in inversion. Hence, the sweep rate need only maintain the inversion layer in equilibrium with the bulk semiconductor. The criterion is then given, for the positive bulk, as

$$\Delta F \approx \left(\frac{N_A V_D}{2q\epsilon_{si}} \right)^{1/2} \frac{\tau_o}{n_i} C_{ox} \frac{dV}{dt}, \quad (61)$$

where ΔF is the difference between the surface quasi- and bulk Fermi level, V_D is the effective diffusion potential, τ_o is the bulk minority-carrier lifetime, and V is the gate voltage.

4.2 Determination of Various Parameters in Density of States Formulation

To calculate the density of states, various needed quantities can be systematically obtained. For instance, from values of the measured capacitance at infinite frequencies, $C_m^{(\infty)}$, the maximum depletion width can be found,

$$W = \left[\frac{C_{ox} - C_M^{(\infty)}}{C_{ox} C_M^{(\infty)}} \right] \epsilon_{si}. \quad (62)$$

Then, for instance, for positive-bulk semiconductors, the doping density, N_A , can be determined via

$$N_A^{-1} \ln (N_A/n_i) = \frac{q^2 W}{4\epsilon_{si} kT} . \quad (63)$$

Given this, one can easily determine the bulk potential, ψ_B , i.e.,

$$\psi_B = \frac{kT}{q} \ln N_A . \quad (64)$$

Then one can determine the one-to-one functional dependence between the actual external potential, V , and the interface potential via Berglund's formula,

$$\psi(V) - \psi_B = \int_{V_{FB}}^V \left[1 - \frac{C_M(\zeta)}{C_{ox}} \right] d\zeta , \quad (65)$$

where the flat-band voltage, V_{FB} , can be obtained from the formula

$$C_{FB}(V_{FB}) = C_{ox} \left[1 - \frac{1}{\sqrt{2}} \left(\frac{C_{ox}}{\epsilon_{si}} \right) L \right]^{-1} , \quad (66)$$

where the Debye length, L , is given by

$$L = \left(\frac{2\epsilon_{si} kT}{q^2 p_0} \right)^{1/2} . \quad (67)$$

At the same time, the mean average charge, which is needed in equation (42) for the variance, can be obtained from the flat-band voltage, i.e.,

$$V_{FB} = \phi_{ms} - \bar{Q} C_{ox}^{-1} , \quad (68)$$

where ϕ_{ms} is the metal-semiconductor work function.

5. CONCLUSION

States associated with the oxide-semiconductor consist of two types, intrinsic and extrinsic. The intrinsic states are manifestations of the heterogeneous nature of the interface, i.e., the loss of both topological and compositional disorder. The extrinsic states, on the other hand, arise due to fluctuations in the interface potential and impurities. This equipotential surface cannot be treated as a flat sheet.

The incorporation of both types of states into a phenomenological treatment based on that of Nicollian and Goetzberger⁸ and Brews¹⁶ will enable one to self-consistently calculate the true density of interface states (without the effects of fluctuations).

⁸E. H. Nicollian and A. Goetzberger, *Bell Syst. Tech. J.*, 45 (1967), 1055.

¹⁶J. R. Brews, *J. Appl. Phys.*, 43 (1972), 2306; 3451.

LITERATURE CITED

- (1) N. J. Chou, J. Electrochem. Soc., 118 (1971), 601.
- (2) F. G. Allen and G. W. Gobeli, Phys. Rev., 127 (1962), 150.
- (3) G. Cluarotti et al, Phys. Rev., B4 (1971), 3398.
- (4) D. Haneman, Phys. Rev., 176 (1968), 705.
- (5) L. F. Wagner and W. E. Spicer, Phys. Rev. Lett., 28 (1972), 1381.
- (6) D. E. Eastman and W. D. Grobman, Phys. Rev. Lett., 28 (1972), 1378.
- (7) J. A. Appelbaum and D. R. Hamann, Phys. Rev. Lett., 31 (1973), 106.
- (8) E. H. Nicollian and A. Goetzberger, Bell Syst. Tech. J., 45 (1967), 1055.
- (9) F. Stern and W. E. Howard, Phys. Rev., 163 (1967), 816; A. B. Fowler, F. F. Fang, W. E. Howard, and P. J. Stiles, Phys. Rev. Lett., 16 (1966), 901.
- (10) D. C. Tsui, Phys. Rev., B4 (1971), 4438; Phys. Rev., B8 (1973), 2657; S. James Allen, D. C. Tsui, and J. V. Dalton, Phys. Rev. Lett., 32 (1974), 107; D. C. Tsui, G. Kaminsky, and P. H. Schmidt, Phys. Rev., B9 (1974), 3524.
- (11) R. Am Abram, J. Phys. Chem., 6 (1973), L379; V. D. S. Shante, Phys. Lett., 43A (1973), 249.
- (12) H. Ibach and J. E. Rowe, Phys. Rev., B9 (1974), 1951.
- (13) A. G. Revesz et al, J. Phys. Chem. Solids, 28 (1967), 197.
- (14) R. Castagne and A. Vapaille, Electronic Letters, 6 (1970), 691.
- (15) M. Kuhn and E. H. Nicollian, J. Electrochem. Soc., 118 (1971), 370.
- (16) J. R. Brews, J. Appl. Phys., 43 (1972), 2306; 3451.
- (17) C. N. Berglund, IEEE Trans. Electron Devices, ED-13 (1966), 701; M. Kuhn, Solid-State Electron., 13 (1970), 873.

LITERATURE CITED (Cont'd)

- (18) W. K. Chu, E. Lugujo, and J. W. Mayer, Appl. Phys. Lett., 24 (1974), 105.
- (19) P. Soven, Phys. Rev., 156 (1967), 809; B. Velicky, S. Kirkpatrick, and H. Ehrenreich, Phys. Rev., 175 (1968), 746.
- (20) M. M. Sokoloski, Bull. Am. Phys. Soc., 20 (1975), 426.
- (21) N. F. Mott and E. A. Davis, Electronic Processes in Non-Crystalline Materials, Clarendon Press, Oxford, England (1971).
- (22) S. C. Moss and J. F. Graczk, Phys. Rev. Lett., 23 (1969), 1167; S. C. Moss and J. F. Graczk, Proceedings of the 10th International Conference on the Physics of Semiconductors, Cambridge, MA (1970), 658.
- (23) R. Castagne and A. Vapaille, Surface Science, 28 (1971), 157; Electron. Lett. 6 (1970), 691; D. J. Silversmith, J. Electrochem. Soc., 119 (1972), 1589.
- (24) H. Scher and E. W. Montroll, Phys. Rev., B12 (1975), 2455; H. E. Boesch, F. B. McLean, J. M. McGarrity, and G. A. Ausman, Jr., IEEE Trans. Nucl. Sci., NS-22 (1975), 2163.
- (25) F. B. McLean, G. A. Ausman, H. E. Boesch, J. M. McGarrity, J. Appl. Phys., 47 (1976), 1529.
- (26) W. Shockley and W. T. Read, Phys. Rev., 87 (1952), 835.
- (27) P. V. Gray and D. M. Brown, Appl. Phys. Lett., 8 (1966), 31; D. M. Brown and P. V. Gray, J. Electrochem. Soc., 115 (1968), 760.
- (28) G. Dedherck, R. Van Overstraeten, and G. Brown, Solid-State Electron., 16 (1973), 1451.
- (29) H. A. Mar and J. Simon, Solid-State Electron., 17 (1974), 131.
- (30) M. Kuhn, Solid-State Electron., 13 (1970), 873.

DISTRIBUTION

COMMANDER
US ARMY MATERIEL DEVELOPMENT
& READINESS COMMAND
500 EISENHOWER AVENUE
ALEXANDRIA, VA 22333
ATTN DRXAM-TL, HQ TECH LIBRARY

COMMANDER
USA RSCH & STD GP (EUR)
BOX 65
FFO NEW YORK 09510
ATTN LTC JAMES M. KENNEDY, JR.
CHIEF, PHYSICS & MATH BRANCH

COMMANDER
USA ARMAMENTS COMMAND
ROCK ISLAND, IL 61201
ATTN AMSAR-ASF, FUZE DIV
ATTN AMSAR-RDF, SYS DEV DIV - FUZES

COMMANDER
USA MISSILE & MUNITIONS CENTER & SCHOOL
REDSTONE ARSENAL, AL 35809
ATTN ATSK-CTD-F

DIRECTOR
DEFENSE COMMUNICATIONS AGENCY
WASHINGTON, DC 20305
ATTN CODE 930, MONTE I. BURGETT, JR

DEFENSE DOCUMENTATION CENTER
CAMERON STATION
ALEXANDRIA, VA 22314
ATTN TC-TCA, (12 COPIES)

DIRECTOR
DEFENSE INTELLIGENCE AGENCY
WASHINGTON, DC 20301
ATTN DS-4A2

DIRECTOR
DEFENSE NUCLEAR AGENCY
WASHINGTON, DC 20305
ATTN DDST
ATTN RAEV
ATTN STTL TECH LIBRARY
ATTN STVL
ATTN RATN

ENERGY RESEARCH & DEVELOPMENT AGENCY
MATERIALS RADIATION EFFECTS BR
DIV OF CONTROLLED THERMONUCLEAR FUSION
WASHINGTON, DC 20545
ATTN MARVIN COHEN

COMMANDER
FIELD COMMAND
DEFENSE NUCLEAR AGENCY
KIRTLAND AFB, NM 87115
ATTN FCPR

DIRECTOR
INTERSERVICE NUCLEAR WEAPONS SCHOOL
KIRTLAND AFB, NM 87115
ATTN DOCUMENT CONTROL

DIRECTOR
JOINT STRATEGIC TARGET
PLANNING STAFF, JCS
OFFUTT AFB
OMAHA, NE 68113
ATTN JLTW-2

CHIEF
LIVERMORE DIVISION, FIELD COMMAND DNA
LAWRENCE LIVERMORE LABORATORY
P.O. BOX 808
LIVERMORE, CA 94550
ATTN DOCUMENT CONTROL FOR L-395
ATTN FCPR

DIRECTOR
NATIONAL SECURITY AGENCY
FT. GEORGE G. MEADE, MD 20755
ATTN O. O. VAN GUNTEN-R-425
ATTN TDL

PROJECT MANAGER
ARMY TACTICAL DATA SYSTEMS
US ARMY ELECTRONICS COMMAND
FORT MONMOUTH, NJ 07703
ATTN DRCPN-TDS-SD
ATTN DWAIN B. HUEWE

COMMANDER
BMD SYSTEM COMMAND
PO BOX 1500
HUNTSVILLE, AL 35807
ATTN BDMSC, TEN, NOAH J. HURST

COMMANDER
FRANKFORD ARSENAL
BRIDGE AND TACONY STREETS
PHILADELPHIA, PA 19137
ATTN SARFA-PCD, MARVIN ELNICK

COMMANDER
PICATINNY ARSENAL
DOVER, NJ 07801
ATTN SARFA-ND-W
ATTN SARFA-TN, BURTON V. FRANKS
ATTN SARFA-ND-N
ATTN SARFA-ND-N-E
ATTN SARFA-FR-E, LOUIS AVRAMI

COMMANDER
REDSTONE SCIENTIFIC INFORMATION CTR
US ARMY MISSILE COMMAND
REDSTONE ARSENAL, AL 35809
ATTN CHIEF, DOCUMENTS

SECRETARY OF THE ARMY
WASHINGTON, DC 20310
ATTN ODUSA OR, DANIEL WILLIARD

COMMANDER
TRASANA
WHITE SANDS MISSILE RANGE, NM 88002
ATTN ATAA-EAC, FRANCIS N. WINANS

DIRECTOR
US ARMY BALLISTIC RESEARCH LABORATORIES
ABERDEEN PROVING GROUND, MD 21005
ATTN DRXBR-AM, W. R. VANANTWERP
ATTN DRXBD-BVL, DAVID L. RIGOTTI
ATTN DRXBR-X, JULIUS J. MESZAROS

COMMANDER
US ARMY COMMUNICATIONS SYSTEMS AGENCY
FORT MONMOUTH, NJ 07703
ATTN SCCM-AD-SV (LIBRARY)

COMMANDER
US ARMY ELECTRONICS COMMAND
FORT MONMOUTH, NJ 07703
ATTN DRSEL-CT-HDK, ABRAHAM E. COHEN
ATTN DRSEL-TL-MD, GERHART K. GAULE
ATTN DRSEL-TL-EN, ROBERT LUX
ATTN DRSEL-GG-TD, W. R. WERK
ATTN DRSEL-PL-ENV, HANS A. BOMKE
ATTN DRSEL-TL-ND, S. KRONENBEY
ATTN DRSEL-TL-IR, EDWIN T. HUNTER

COMMANDER-IN-CHIEF
US ARMY EUROPE AND SEVENTH ARMY
APO NEW YORK 09403
ATTN ODCSE-E, AEAGE-PI

COMMANDER
US ARMY MISSILE COMMAND
REDSTONE ARSENAL, AL 35809
ATTN DRCPM-PE-EA, WALLACE C. WAGNER
ATTN DRSMI-RGD, VICTOR W. RUWE
ATTN DRSMI-RRR, FAISON P. GIBSON
ATTN DRCPM-MTI, CPT JOE A. SIMS
ATTN DRSMI-RGI, HUGH GREEN
ATTN DRCPM-LCEX, HOWARD H. HENRIKSEN

COMMANDER
US ARMY MOBILITY EQUIP P&D CTR
FORT BELVOIR, VA 22060
ATTN STSFB-MW, JOHN W. BOND, JR.

CHIEF
US ARMY NUC AND CHEMICAL SURETY GP
BLDG, 2073, NORTH AREA
FT. BELVOIR, VA 22060
ATTN MOSG-ND, MAJ SIDNEY W. WINSLOW

COMMANDER
US ARMY NUCLEAR AGENCY
FORT BLISS, TX 79916
ATTN ATCN-W, LTC LEONARD A. SLUGA

COMMANDER
US ARMY RESEARCH OFFICE
PO BOX 12211
RESEARCH TRIANGLE PARK, NC 27709
ATTN R. LONTZ

COMMANDER
US ARMY TEST AND EVALUATION COMMAND
ABERDEEN PROVING GROUND, MD 21005
ATTN DRSTE-EL, P. I. KOLCHIN
ATTN DRSTE-MB, R. P. GALASSO

CHIEF OF NAVAL RESEARCH
NAVY DEPARTMENT
ARLINGTON, VA 22217
ATTN CODE 421, DORAN W. FADGETT
ATTN CODE 427

COMMANDER
NAVAL ELECTRONIC SYSTEMS COMMAND
HEADQUARTERS
WASHINGTON, DC 20360
ATTN FME 117-21
ATTN ELIX 05323, CLEVELAND F. WATKINS
ATTN CODE 504510

DISTRIBUTION (Cont'd)

COMMANDING OFFICER
NAVAL INTELLIGENCE SUPPORT CENTER
4301 SUITLAND ROAD, BLDG 5
WASHINGTON, DC 20390
ATTN F. ALEXANDER

DIRECTOR
NAVAL RESEARCH LABORATORY
WASHINGTON, DC 20375
ATTN CODE 6631, JAMES C. RITTER
ATTN CODE 4004, EMANUEL L. BRANCATO
ATTN CODE 2627, DORIS R. POLEN
ATTN CODE 7701, JACK D. BROWN
ATTN CODE 5216, HAROLD L. HUGHES
ATTN CODE 5210, JOHN E. DAVEY
ATTN CODE 601, E. WOLICKI

COMMANDER
NAVAL SEA SYSTEMS COMMAND
NAVY DEPARTMENT
WASHINGTON, DC 20362
ATTN SEA-9931, RILEY B. LANE
ATTN SEA-9931, SAMUEL A. BARHAM

COMMANDER
NAVAL SHIP ENGINEERING CENTER
CENTER BUILDING
HYATTSVILLE, MD 20782
ATTN CODE 6174D2, EDWARD F. DUFFY

COMMANDER
NAVAL SURFACE WEAPONS CENTER
WHITE OAK, SILVER SPRING, MD 20910
ATTN CODE WA501, NAVY MUC PRGMS OFF
ATTN CODE WA50, JOHN H. MALLOY

COMMANDER
NAVAL SURFACE WEAPONS CENTER
DAHLGREN LABORATORY
DAHLGREN, VA 22448
ATTN WILLIAM H. HOLT

COMMANDER
NAVAL WEAPONS CENTER
CHINA LAKE, CA 93555
ATTN CODE 533, TECHNICAL LIBRARY

COMMANDING OFFICER
NAVAL WEAPONS SUPPORT CENTER
CRANE, IN 47522
ATTN CODE 70242, JOSEPH A. MUNARIN
ATTN CODE 7024, JAMES RAMSEY

COMMANDING OFFICER
NUCLEAR WEAPONS TRAINING CENTER PACIFIC
NAVAL AIR STATION, NORTH ISLAND
SAN DIEGO, CA 92135
ATTN CODE 50

DIRECTOR
STRATEGIC SYSTEMS PROJECT OFFICE
NAVY DEPARTMENT
WASHINGTON, DC 20376
ATTN NSP-2342, RICHARD L. COLEMAN

GEOPHYSICS LABORATORY
HANSCOM AFB, MA 01731
ATTN J. EMEY CORMIER
ATTN LQR, EDWARD A. BURKE

AF INSTITUTE OF TECHNOLOGY, AU
WRIGHT-PATTERSON AFB, OH 45433
ATTN ENP, CHARLES J. BRIDGMAN

AF MATERIALS LABORATORY, AFSC
WRIGHT-PATTERSON AFB, OH 45433
ATTN LTE

AF WEAPONS LABORATORY, AFSC
KIRTLAND AFB, NM 87117
ATTN SAT
ATTN ELA
ATTN SAB

AFTAC
PATRICK AFB, FL 32925
ATTN TAB

HEADQUARTERS
ELECTRONIC SYSTEMS DIVISION, (AFSC)
L. G. HANSCOM FIELD
BEDFORD, MA 01730
ATTN YSEV, LTC DAVID C. SPARKS

COMMANDER
FOREIGN TECHNOLOGY DIVISION, AFSC
WRIGHT-PATTERSON AFB, OH 45433
ATTN ETET, CAPT RICHARD C. HUSEMANN

SAMSO/DY
POST OFFICE BOX 92960
WORLDWAY POSTAL CENTER
LOS ANGELES, CA 90009
ATTN DYS, CAPT WAYNE SCHOBEL
ATTN DYS, MAJ LARRY A. DARDA

SAMSO/IN
POST OFFICE BOX 92960
WORLDWAY POSTAL CENTER
LOS ANGELES, CA 90009
ATTN IND, T. J. JULY

SAMSO/MN
NORTON AFB, CA 92409
ATTN MNNG, CAPT DAVID J. STROBEL

SAMSO/RS
POST OFFICE BOX 92960
WORLDWAY POSTAL CENTER
LOS ANGELES, CA 90009
ATTN RSE
ATTN RSSE, LTC KENNETH L. GILBERT

SAMSO/SZ
POST OFFICE BOX 92960
WORLDWAY POSTAL CENTER
LOS ANGELES, CA 90009
ATTN SZJ, CAPT JOHN H. SALCH

SAMSO/YD
POST OFFICE BOX 92960
WORLDWAY POSTAL CENTER
LOS ANGELES, CA 90009
ATTN YDD, MAJ M. F. SCHNEIDER

COMMANDER IN CHIEF
STRATEGIC AIR COMMAND
OFFUTT AFB, NE 68113
ATTN NRI-STINFO LIBRARY
ATTN XFFS, MAJ BRIAN STEPHAN

LOS ALAMOS SCIENTIFIC LABORATORY
P.O. BOX 1663
LOS ALAMOS, NM 87544
ATTN MARVIN M. HOFFMAN
ATTN J. ARTHUR FREED
ATTN BRUCE W. NOEL

SANDIA LABORATORIES
LIVERMORE LABORATORY
PO BOX 969
LIVERMORE, CA 94550
ATTN THEODORE A. DELLIN
ATTN P. L. MATTERN

SANDIA LABORATORIES
PO BOX 5800
ALBUQUERQUE, NM 87115
ATTN 3141 SANDIA RPT COLL
ATTN ORG 2110, J. A. HOOD
ATTN ORG 1933, F. N. COPPAGE
ATTN JACK V. WALKER, 5220
ATTN R. C. HUGHES
ATTN HOWARD SANDER
ATTN DIV 5231, JAMES H. BENKEN

US ENERGY RSCH & DEV ADMIN
ALBUQUERQUE OPERATIONS OFFICE
PO BOX 5400
ALBUQUERQUE, NM 87115
ATTN WSSB

UNIVERSITY OF CALIFORNIA
LAWRENCE LIVERMORE LABORATORY
PO BOX 808
LIVERMORE, CA 94550
ATTN DONALD J. MEERER, L-545
ATTN HANS KRUGER, L-96
ATTN TECH INFO DEPT, L-3
ATTN LAWRENCE CLELAND, L-156
ATTN RONALD L. OTT, L-531
ATTN JOSEPH E. KELLER, JR., L-125
ATTN FREDERICK R. KOVAR, L-31

CENTRAL INTELLIGENCE AGENCY
ATTN RD/SI, RM 5G48, HQ BLDG
WASHINGTON, DC 20505
ATTN ALICE A. PADGETT

DEPARTMENT OF COMMERCE
NATIONAL BUREAU OF STANDARDS
WASHINGTON, DC 20234
ATTN JUDSON C. FRENCH
ATTN APPL RAD DIV
ROBERT C. PLACIUS
ATTN SEMICONDUCTOR TECHNOLOGY,
W. M. BULLIS
ATTN K. F. GALLAWAY

AEROJET ELECTRO-SYSTEMS CO DIV
AEROJET-GENERAL CORPORATION
PO BOX 296
AZUSA, CA 91702
ATTN THOMAS D. HANSCOME

AERONUTRONIC FORD CORPORATION
AEROSPACE & COMMUNICATIONS OPS
AERONUTRONIC DIVISION
FORD & JAMBOREE ROADS
NEWPORT BEACH, CA 92663
ATTN KEN C. ATTINGER
ATTN TECH INFO SECTION

DISTRIBUTION (Cont'd)

AERONUTRONIC FORD CORPORATION
WESTERN DEVELOPMENT LABORATORIES DIV
3939 FABIAN WAY
PALO ALTO, CA 94303
ATTN SAMUEL R. CRAWFORD, MS 531
ATTN DONALD R. MCMORROW, MS C30

AFROSPACE CORPORATION
PO BOX 92957
LOS ANGELES, CA 90009
ATTN IRVING M. GARFUNKEL
ATTN JULIAN REINHIMER
ATTN LIBRARY
ATTN MELVIN J. BERNSTEIN
ATTN WILLIAM W. WILLIS
ATTN L. W. AUKERMAN

AVCO RESEARCH & SYSTEMS GROUP
201 LOWELL STREET
WILMINGTON, MA 01887
ATTN RESEARCH LIBRARY, A830, RM 7201

BDM CORPORATION, THE
PO BOX 9274
ALBUQUERQUE INTERNATIONAL
ALBUQUERQUE, NM 87119
ATTN T. H. NEIGHBORS

BENDIX CORPORATION, THE
COMMUNICATION DIVISION
EAST JOPPA ROAD - TOWSON
BALTIMORE, MD 21204
ATTN DOCUMENT CONTROL

BENDIX CORPORATION, THE
RESEARCH LABORATORIES DIV
BENDIX CENTER
SOUTHFIELD, MI 48075
ATTN MGR PRGM DEV,
DONALD J. NIEHAUS

BOEING COMPANY, THE
PO BOX 3707
SEATTLE, WA 98124
ATTN HOWARD W. WICKLEIN, MS 17-11
ATTN DAVID DYE, MS 87-75
ATTN AEROSPACE LIBRARY
ATTN ROBERT S. CALDWELL, 2R-00

BOOZ-ALLEN AND HAMILTON, INC.
106 APPLE STREET
NEW SHREWSBURY, NJ 07724
ATTN R. J. CHRISNER

CALIFORNIA INSTITUTE OF TECHNOLOGY
JET PROPULSION LABORATORY
4800 OAK GROVE
PASADENA, CA 91103
ATTN A. G. STANLEY
ATTN J. BRYDEN

CHARLES STARK DRAPER LABORATORY INC.
68 ALBANY STREET
CAMBRIDGE, MA 02139
ATTN KENNETH FERTIG
ATTN RICHARD G. HALTMAIER
ATTN PAUL R. KELLY

COMPUTER SCIENCES CORPORATION
201 LA VETA DRIVE, NE
ALBUQUERQUE, NM 87108
ATTN RICHARD H. DICKHAUT

C. T. SAH ASSOCIATES
PO BOX 364
URBANA, IL 61801
ATTN C. T. SAH

CUTLER-HAMMER, INC.
AIL DIVISION
COMAC ROAD
DEER PARK, NY 11729
ATTN CENTRAL TECH FILES,
ANN ANTHONY

DIKEWOOD CORPORATION, THE
1009 BRADBURY DRIVE, SE
UNIVERSITY RESEARCH PARK
ALBUQUERQUE, NM 87106
ATTN L. WAYNE DAVIS

E-SYSTEMS, INC.
GREENVILLE DIVISION
PO BOX 1056
GREENVILLE, TX 75401
ATTN LIBRARY 8-50100

EFFECTS TECHNOLOGY, INC.
5383 HOLISTER AVENUE
SANTA BARBARA, CA 93105
ATTN EDWARD JOHN STEELE

ELECTRONICS TECHNOLOGY LABORATORY
ENGINEERING EXPERIMENT STATION
GEORGIA INSTITUTE OF TECHNOLOGY
ATLANTA, GA 30332
ATTN R. CURRY

EXPERIMENTAL AND MATHEMATICAL
PHYSICS CONSULTANTS
P. O. BOX 66331
LOS ANGELES, CA 90066
ATTN THOMAS M. JORDAN

FAIRCHILD CAMERA AND
INSTRUMENT CORPORATION
464 ELLIS STREET
MOUNTAIN VIEW, CA 94040
ATTN 2-233, MR. DAVID K. MYERS

FAIRCHILD INDUSTRIES, INC.
SHERMAN FAIRCHILD TECHNOLOGY CENTER
20301 CENTURY BOULEVARD
GERMANTOWN, MD 20767
ATTN MGR CONFIG DATA & STANDARDS

UNIVERSITY OF FLORIDA
231 AEROSPACE BLDG
GAINESVILLE, FL 32611
ATTN D. P. KENNEDY

FRANKLIN INSTITUTE, THE
20TH STREET AND PARKWAY
PHILADELPHIA, PA 19103
ATTN FAMIE H. THOMPSON

GENERAL DYNAMICS CORP
ELECTRONICS DIV ORLANDO OPERATIONS
PO BOX 2566
ORLANDO, FL 32802
ATTN D. W. COLEMAN

GENERAL ELECTRIC COMPANY
SPACE DIVISION
VALLEY FORGE SPACE CENTER
P.O. BOX 8555
PHILADELPHIA, PA 19101
ATTN JAMES P. SPRATT
ATTN LARRY I. CHASEN
ATTN JOSEPH C. PEDEN, CCF 8301
ATTN JOHN L. ANDREWS
ATTN CSP 6-7, RICHARD C. FRIES

GENERAL ELECTRIC COMPANY
RE-ENTRY & ENVIRONMENTAL SYSTEMS DIV
PO BOX 7722
3198 CHESTNUT STREET
PHILADELPHIA, PA 19101
ATTN ROBERT V. BENEDICT

GENERAL ELECTRIC COMPANY
ORDNANCE SYSTEMS
100 PLASTICS AVENUE
PITTSFIELD, MA 01201
ATTN JOSEPH J. REIDL

GENERAL ELECTRIC COMPANY
TEMPO-CENTER FOR ADVANCED STUDIES
816 STATE STREET (PO DRAWER QQ)
SANTA BARBARA, CA 93102

ATTN DASIAC
ATTN ROYDEN R. RUTHERFORD
ATTN M ESPIG

GENERAL ELECTRIC COMPANY
PO BOX 1122
SYRACUSE, NY 13201
ATTN CSP 6-7, RICHARD C. FRIES
ATTN CSP 0-7, L. H. DEE

GENERAL ELECTRIC COMPANY
AIRCRAFT ENGINE GROUP
EVENDALE PLANT
CINCINNATI, OH 45215
ATTN JOHN A. ELLERHORST, E2

GENERAL ELECTRIC COMPANY
AEROSPACE ELECTRONICS SYSTEMS
FRENCH ROAD
UTICA, NY 13503
ATTN W. J. PATTERSON, DROP 233

GENERAL ELECTRIC COMPANY
PO BOX 5000
BINGHAMTON, NY 13902
ATTN DIVID W. PEPIN, DROP 160

GENERAL ELECTRIC COMPANY-TEMPO
ATTN: DASIAC
C/O DEFENSE NUCLEAR AGENCY
WASHINGTON, DC 20305
ATTN WILLIAM ALFONTE

DISTRIBUTION (Cont'd)

GENERAL RESEARCH CORPORATION
P.O. BOX 3587
SANTA BARBARA, CA 93105
ATTN ROBERT D. HILL

GRUMMAN AEROSPACE CORPORATION
SOUTH OYSTER BAY ROAD
BETHPAGE, NY 11714
ATTN JERRY ROGERS, DEPT 533

GTE SYLVANIA, INC.
ELECTRONICS SYSTEMS GRP-EASTERN DIV
77 A STREET
NEEDHAM, MA 02194
ATTN CHARLES A. THORNHILL, LIBRARIAN
ATTN LEONARD L. BLAISDELL
ATTN JAMES A. WALDON

GTE SYLVANIA, INC.
189 B STREET
NEEDHAM HEIGHTS, MA 02194
ATTN CHARLES H. RAMSBOTTOM
ATTN HERBERT A. ULLMAN
ATTN H & V GROUP, MARIO A. NUREFORA
ATTN PAUL B. FREDRICKSON

HARRIS CORPORATION
HARRIS SEMICONDUCTOR DIVISION
P.O. BOX 583
MELBOURNE, FL 32901
ATTN C. P. DAVIS, MS 17-220
ATTN T. CLARK, MS 4040
ATTN WAYNE E. ABARE, MS 16-111

HAZELTINE CORPORATION
PULASKI ROAD
GREEN LAWN, NY 11740
ATTN TECH INFO CTR, M. WAITE

HONEYWELL INCORPORATED
GOVERNMENT AND AERONAUTICAL
PRODUCTS DIVISION
2600 RIDGEWAY PARKWAY
MINNEAPOLIS, MN 55413
ATTN RONALD R. JOHNSON, A1622

HONEYWELL INCORPORATED
AEROSPACE DIVISION
13350 US HIGHWAY 19
ST. PETERSBURG, FL 33733
ATTN MS 725-J, STACEY H. GRAFF

HONEYWELL INCORPORATED
RADIATION CENTER
2 FORBES ROAD
LEXINGTON, MA 02173
ATTN TECHNICAL LIBRARY

HUGHES AIRCRAFT COMPANY
CENTINELA & TEALF
CULVER CITY, CA 90230
ATTN M.S. D157, KEN WALKER
ATTN B. W. CAMPBELL, M.S. 6-E110
ATTN DAN BINDER, MS 6-D147

HUGHES AIRCRAFT COMPANY
SPACE SYSTEMS DIVISION
P.O. BOX 92919
LOS ANGELES, CA 90009
ATTN WILLIAM W. SCOTT, MS A1080
ATTN EDWARD C. SMITH, MS A620

HUGHES AIRCRAFT COMPANY
500 SUPERIOR AVE
NEWPORT BEACH, CA 92663
ATTN KENNETH AUBUCHON
ATTN ELI HARARI

IBM CORPORATION
ROUTE 17C
OWEGO, NY 13827
ATTN FRANK FRANKOVSKY

INTELCOR RAD TECH
P.O. BOX 81087
SAN DIEGO, CA 92138
ATTN ROLAND LEADON
ATTN T. M. PLANAGAN

ION PHYSICS CORPORATION
SOUTH BEDFORD STREET
BURLINGTON, MA 01803
ATTN ROBERT D. EVANS

IRT CORPORATION
PO BOX 81087
SAN DIEGO, CA 92138
ATTN MDC
ATTN JAMES A. NABER
ATTN RALPH H. STAHL
ATTN R. L. MERTZ

KAMAN SCIENCES CORPORATION
P.O. BOX 7463
COLORADO SPRINGS, CO 80933
ATTN DONALD H. BRYCE
ATTN ALBERT P. BRIDGES
ATTN WALTER E. WARE

LEHIGH UNIVERSITY
MATERIALS RESEARCH CENTER
BETHLEHEM, PA 18015
ATTN S. R. BUTLER
ATTN F. J. FEIGL
ATTN F. M. FOWKES

LITTON SYSTEMS, INC.
GUIDANCE & CONTROL SYSTEMS DIVISION
5500 CANOGA AVENUE
WOODLAND HILLS, CA 91364
ATTN VAL J. ASHBY, MS 67
ATTN JOHN P. RETZLER

LOCKHEED MISSILES AND SPACE
COMPANY, INC.
P.O. BOX 504
SUNNYVALE, CA 94088
ATTN G. F. HEATH, D/81-14
ATTN BENJAMIN T. KIMURA,
DEPT 81-14, BLDG 154
ATTN EDWIN A. SMITH, DEPT 85-85
ATTN PHILIP J. HART, DEPT 81-14
ATTN L. ROSSI, DEPT 81-64
ATTN DEPT 81-01, G. H. MORRIS

LOCKHEED MISSILES AND SPACE COMPANY
3251 HANOVER STREET
PALO ALTO, CA 94304
ATTN TECH INFO CTR D/COLL
LTV AEROSPACE CORPORATION
VOUGHT SYSTEMS DIVISION
P.O. BOX 6267
DALLAS, TX 75222
ATTN TECHNICAL DATA CENTER

LTV AEROSPACE CORPORATION
PO BOX 5907
DALLAS, TX 75222
ATTN TECHNICAL DATA CTR

M.I.T. LINCOLN LABORATORY
P.O. BOX 73
LEXINGTON, MA 02173
ATTN LEONA LOUGHLIN, LIBRARIAN A-062

MARTIN MARIETTA AEROSPACE
ORLANDO DIVISION
P.O. BOX 5837
ORLANDO, FL 32805
ATTN MONA C. GRIFFITH, LIB MF-30
ATTN WILLIAM W. MEAS, MF-413

MARTIN MARIETTA CORPORATION
DENVER DIVISION
PO BOX 179
DENVER, CO 80201
ATTN J. E. GOODWIN, MAIL 0452
ATTN RESEARCH LIB, 6617, J. F. MCKEE
ATTN BEN T. GRAHAM, MS FO-454

MCDONNELL DOUGLAS CORPORATION
POST OFFICE BOX 516
ST. LOUIS, MO 63166
ATTN TECHNICAL LIBRARY

MCDONNELL DOUGLAS CORPORATION
5301 BOLSA AVENUE
HUNTINGTON BEACH, CA 92647
ATTN STANLEY SCHNEIDER

MISSION RESEARCH CORPORATION
735 STATE STREET
SANTA BARBARA, CA 93101
ATTN WILLIAM C. HART

MISSION RESEARCH CORPORATION-SAN DIEGO
7650 CONVOY COURT
SAN DIEGO, CA 92111
ATTN V. A. J. VAN LINT

NATIONAL ACADEMY OF SCIENCES
2101 CONSTITUTION AVE, NW
WASHINGTON, DC 20418
ATTN DR. R. S. SHANE,
NAT MATERIALS ADVISORY BOARD

UNIVERSITY OF NEW MEXICO
DEPT OF CAMPUS SECURITY AND POLICE
1821 ROMA NE
ALBUQUERQUE, NM 87106
ATTN W. W. GRANNEMANN

NORTHROP CORPORATION
ELECTRONIC DIVISION
1 RESEARCH PARK
PALOS VERDES PENINSULA, CA 90274
ATTN VINCENT R. DEMARTINO
ATTN BOYCE T. AHLFORT
ATTN GEORGE H. TOWNER

NORTHROP CORPORATION
NORTHROP RESEARCH AND TECHNOLOGY CENTER
3401 WEST BROADWAY
HAWTHORNE, CA 90250
ATTN DAVID N. POCOCK
ATTN JOSEPH R. SKOUR

DISTRIBUTION (Cont'd)

PHYSICS INTERNATIONAL COMPANY
2700 MERCED STREET
SAN LEANDRO, CA 94577
ATTN CHARLES H. STALLINGS
ATTN JOHN H. HUNTINGTON

PRINCETON UNIVERSITY
DEPT OF AEROSPACE &
MECHANICAL SCIENCES
PRINCETON, NJ 08940
ATTN BARRIE S. H. ROYCE

R & D ASSOCIATES
PO BOX 9695
MARINA DEL REY, CA 90291
ATTN S. CLAY ROGERS

RAYTHEON COMPANY
HARTWELL ROAD
BEDFORD, MA 01730
ATTN GAJANAN H. JOSHI,
RADAR SYS LAB

RCA CORPORATION
GOVERNMENT & COMMERCIAL SYSTEMS
ASTRO ELECTRONICS DIVISION
PO BOX 800, LOCUST CORNER
PRINCETON, NJ 08540
ATTN GEORGE J. BRUCKER

RCA CORPORATION
DAVID SARNOFF RESEARCH CENTER
W. WINDSOR TWP
201 WASHINGTON ROAD, PO BOX 432
PRINCETON, NJ 08540
ATTN K. H. ZAININGER
ATTN R. J. POWELL

RENSSELAER POLYTECHNIC INSTITUTE
PO BOX 965
TROY, NY 12181
ATTN RONALD J. GUTMANN

RESEARCH TRIANGLE INSTITUTE
PO BOX 12194
RESEARCH TRIANGLE PARK, NC 27709
ATTN ENG DIV, MAYRANT SIMONS, JR.

ROCKWELL INTERNATIONAL CORPORATION
3370 MIRALOMA AVENUE
ANAHEIM, CA 92803
ATTN K. F. HULL
ATTN JAMES E. BELL, HA10
ATTN DONALD J. STEVENS, FA70
ATTN GEORGE C. MESSENGER, FB61

ROCKWELL INTERNATIONAL CORPORATION
ELECTRONICS OPERATIONS
COLLINS RADIO GROUP
5225 C. AVE NE
CEDAR RAPIDS, IA 52406
ATTN DENNIS SUTHERLAND

SANDERS ASSOCIATES, INC.
95 CANAL STREET
NASHUA, NH 03060
ATTN M. L. AITEL, NCA 1-3236

SCIENCE APPLICATIONS, INC.
1651 OLD MEADOW ROAD
MCLEAN, VA 22101
ATTN WILLIAM L. CHADSEY

SCIENCE APPLICATIONS, INC.
PO BOX 2351
LA JOLLA, CA 92038
ATTN LARRY SCOTT
ATTN J. ROBERT BEYSTER

SCIENCE APPLICATIONS, INC.
HUNTSVILLE DIVISION
2109 W. CLINTON AVENUE
SUITE 700
HUNTSVILLE, AL 35805
ATTN NOEL R. BYRN

SCIENCE APPLICATIONS, INC.
2680 HANOVER STREET
PALO ALTO, CA 94303
ATTN CHARLES STEVENS

SIMULATION PHYSICS, INC.
41 "B" STREET
BURLINGTON, MA 01803
ATTN ROGER G. LITTLE

SINGER COMPANY, THE
1150 MC BRIDE AVENUE
LITTLE FALLS, NJ 07424
ATTN IRWIN GOLDMAN, ENG MANAGEMENT

SINGER COMPANY (DATA SYSTEMS), THE
150 TOTOWA ROAD
WAYNE, NJ 07470
ATTN TECH INFO CENTER

SPERRY RAND CORPORATION
SPERRY DIVISION
SPERRY GYROSCOPE DIVISION
SPERRY MANAGEMENT DIVISION
MARCUS AVENUE
GREAT NECK, NY 11020
ATTN PAUL MARRAFFINO
ATTN CHARLES L. CRAIG EV

STANFORD RESEARCH INSTITUTE
333 RAVENSWOOD AVENUE
MENLOW PARK, CA 94025
ATTN MR. PHILIP DOLAN
ATTN ROBERT A. ARMISTEAD

STANFORD RESEARCH INSTITUTE
306 WYNN DRIVE, N. W.
HUNTSVILLE, AL 35805
ATTN MACPHERSON MORGAN

SUNDSTRAND CORPORATION
4751 HARRISON AVENUE
ROCKFORD, IL 61101
ATTN DEPT 763SW, CURTIS WHITE

TEXAS INSTRUMENTS, INC.
P.O. BOX 5474
DALLAS, TX 75222
ATTN DONALD J. MANUS, MS 72

TRW SYSTEMS GROUP
ONE SPACE PARK
REDONDO BEACH, CA 90278
ATTN R. D. LOVELAND, R1-1028
ATTN A. A. WITTELES, MS R1-1120
ATTN TECH INFO CENTER/S-1930
ATTN A. M. LIEBSCHUTZ R1-1162
ATTN AARON H. NAREVSKY, R1-2144
ATTN RICHARD H. KINGSLAND, R1-2154
ATTN JERRY I. LUBELL
ATTN LILLIAN D. SINGLETARY, R1/1070
ATTN WILLIAM H. ROBINETTE, JR.
ATTN PAUL MOLMUD, R1-1196
ATTN ALLAN ANDERMAN, R1-1132

TRW SYSTEMS GROUP
SAN BERNARDINO OPERATIONS
PO BOX 1310
SAN BERNARDINO, CA 92402
ATTN EARL W. ALLEN
ATTN JOHN E. DAHNKE
ATTN H. S. JENSEN

WESTINGHOUSE ELECTRIC CORPORATION
DEFENSE AND ELECTRONIC SYSTEMS CENTER
P.O. BOX 1693
FRIENDSHIP INTERNATIONAL AIRPORT
BALTIMORE, MD 21203
ATTN HENRY P. KALAPACA, MS 3525

WESTINGHOUSE ELECTRIC CORPORATION
RESEARCH AND DEVELOPMENT CENTER
1310 BEULAH ROAD, CHURCHILL BOROUGH
PITTSBURGH, PA 15235
ATTN WILLIAM E. NEWELL

COMMANDER
HARRY DIAMOND LABORATORIES
2800 POWDER MILL RD
ADELPHI, MD 20783

ATTN MCGREGOR, THOMAS, COL, COMMANDER
FLYER, I.N./LANDIS, F.F./
SOMMER, H./OSWALD, F. P.

ATTN CARTER, W.W., DR., TECHNICAL
DIRECTOR/MARCUS, S.M.

ATTN KIMMEL, S., PAO
ATTN CHIEF, 0021
ATTN CHIEF, 0022
ATTN CHIEF, LAB 100
ATTN CHIEF, LAB 200
ATTN CHIEF, LAB 300
ATTN CHIEF, LAB 400
ATTN CHIEF, LAB 500
ATTN CHIEF, LAB 600
ATTN CHIEF, DIV 700
ATTN CHIEF, DIV 800
ATTN CHIEF, LAB 900
ATTN CHIEF, LAB 1000

ATTN RECORD COPY, BR 041
ATTN HDL LIBRARY (3 COPIES)
ATTN CHAIRMAN, EDITORIAL COMMITTEE
ATTN CHIEF, 047

ATTN TECH REPORTS, 013
ATTN PATENT LAW BRANCH, 071
ATTN MCLAUGHLIN, P.W., 741
ATTN LANHAM, C., 0021
ATTN CHIEF, BR 230

ATTN ROSADO, J. A., 240
ATTN CHIEF, BR 280
ATTN CALDWELL, P. A., 290
ATTN SCHALLHORN, D. R., 230
ATTN OLDFHAM, T. R., 230

ATTN SCHARF, W. D., 230
ATTN BOESCH, H. E., JR. 280
ATTN WINOKUR, P. S., 280
ATTN WIMENITZ, F. N., 0024
ATTN MCGARRITY, J. M., 280

ATTN SOKOLOSKI, M. M., 0021 (20 COPIES)
ATTN AUSMAN, G. A., 210
ATTN MCLEAN, F. H., 280